Space-Time Spreading and Transmit Diversity for DS-CDMA Systems over Fading Channels

Mohamed AlJerjawi

A Thesis

in

The Department

of

Electrical and Computer Engineering

Presented in Partial Fulfillment of the Requirements

for the Degree of Master of Applied Science at

Concordia University

Montréal, Québec, Canada

April 2006

Your file Votre référence
ISBN: 0-494-14252-9
Our file Notre référence
ISBN: 0-494-14252-9

ABSTRACT

Space-Time Spreading and Transmit Diversity for DS-CDMA Systems over Fading Channels

Mohamed AlJerjawi

The application of space-time coding in wireless communication systems has shown to improve the quality of the received signal at the mobile user by placing the spatial diversity at the base station. In this thesis, we propose a simple space-time spreading scheme for code-division multiple-access (CDMA) systems over fast-fading channels. The proposed transmit diversity scheme is based on two transmit and M receive antennas and is suitable for Rayleigh fast-fading channels. In this we employ orthogonal spreading codes to exploit the time diversity introduced by the channel, and hence a two-fold of the diversity order obtained using existing space-time spreading schemes is achieved. Nevertheless, for slowly-fading channels, we show that the proposed coding scheme reduces to existing schemes introduced in the literature with no performance degradation. Then, we examine the effect of using nonorthogonal spreading codes on the receiver performance. Our results show that using a simple adaptive decoder, based on the minimum mean-squared error (MMSE) criterion, the diversity order is still maintained and only a small loss in the signal-to noise ratio (SNR) is incurred relative to the ideal case with orthogonal codes. Furthermore, for the single user case, and using orthogonal spreading codes,

the underlying transmit diversity scheme is analyzed over fast-fading channels. On the other hand, for the multiuser case we derive closed form expressions for the probability of bit error for a receiver that employs the decorrelator multiuser detector for both fast and slow-fading channels. These results prove that the diversity order is maintained as a linear inverse relationship with the average SNR per channel. We verify the accuracy of our analytical results by comparison with simulations for different system loads. We show that the diversity order is maintained even for a heavily loaded system.

Finally, for a system with N transmit and M receive antennas, we demonstrate that regardless of the system load, the full diversity order of NM is always maintained and only an SNR loss is incurred on the slowly-fading channel when using a decorrelator detector. This SNR degradation is shown to be a function only of the number of users and independent of the number of transmit and/or receive antennas. Using our theoretical results, we show that the loss in SNR from the single-user bound is upper bounded by $10log(C/2)$ where (C) represents the sum of the two consecutive diagonal elements of the inverse of the cross-correlation matrix for the user under consideration.

To my parents, sisters and my homeland

ACKNOWLEDGEMENTS

First and foremost, I wish to express my greatest gratitude and thanks to my mentor, Dr. Walaa A. Hamouda for all the generous help and guidance he provided for this research. His precious time and devotion to responding to my questions, was of great help and made this research possible. His trial has always been in place to keep the research environment friendly and stress-free. Without his exceptional patience and selflessness and dedication to his students this thesis would not have come into its entirety.

I would like also to extend my appreciation to my dearest parents and sisters for their great sacrifice, support and patience which made my study much easier to achieve and a memorable experience.

Finally, I want to thank my friends who encouraged me throughout my study in Concordia University.

Mohamed AlJerjawi

Montrèal

April 2006

TABLE OF CONTENTS

LIST OF TABLES

LIST OF FIGURES

LIST OF ACRONYMS

BER	bit error rate
BPSK	binary phase-shift keying
DS-CDMA	direct sequence code division multiple access
FDMA	frequency division multiple access
MMSE	minimum mean-squared-error
NLMS	normalized least mean square
MAI	multiple access interference
MLS	maximum likelihood sequence
MUD	multiuser detection
SIC	successive interference cancellation
SIR	signal to interference ratio
SNR	signal to noise ratio
STBC	space-time block codes
STC	space-time codes
STTC	space-time trellis codes
TDMA	time division multiple access

Chapter 1

Introduction

1.1 CDMA Communications

The area of wireless communications for mobile telephone and data transmission is currently undergoing very rapid development. Many of the emerging wireless systems will incorporate considerable signal processing intelligence in order to provide advanced services such as multimedia transmission. Since the bandwidth is a valuable resource, the problem of interest is to be able to accommodate as many users as can be reliably demodulated for a given bandwidth. In order to make an optimal use of the available bandwidth and to provide maximal flexibility, many wireless systems operate as multiple-access systems, in which channel bandwidth is shared by many users on a random-access basis.

Code-division multiple access (CDMA) is one of the several methods of multiplexing wireless users that has become very popular in recent years. In CDMA, users are multiplexed by distinct codes rather than by orthogonal frequency bands, as in frequency-division multiple access (FDMA), or by orthogonal time slots, as in time-division multiple access (TDMA). In CDMA, all users can transmit at the same time, each being allocated the entire available frequency spectrum. Hence, CDMA is also known as spread-spectrum multiple access (SSMA), or simply by spread-spectrum communications. CDMA is a promising technology for wireless environments with multiple simultaneous transmission because of several features: asynchronous multiple access, robustness to frequency selective fading, and multipath combining.

Three major factors that limit the performance of CDMA systems in the cellular channel are multiple access interference (MAI), the near-far effect, and multipath fading. In DS-CDMA systems, the users are multiplexed by distinct code waveforms and MAI is caused by non-orthogonal code sequences. Considering cellular mobile systems, mobile units transmit independently so that their signals arrive asynchronously at the base station. Since their relative time delays are randomly distributed, the cross-correlation between the received signals coming from different users is nonzero.

To achieve a low level of interference, the assigned signatures need to have low cross-correlations for all relative time delays. A low cross-correlation between

signature waveforms is obtained by designing a set of special random sequences. However, there is no known set of code sequences that is completely orthogonal when used in an asynchronous system. The non-orthogonal components of signals of other users will appear in the demodulated desired signal as interference. If the conventional receiver is used in such a system, the number of users is limited by the interference coming from other users. In conclusion, the capacity of DS-CDMA systems is interference limited, as opposed to other multiple access schemes which are bandwidth limited, and the performance of the system for all users considerably degrades as the number of active users increases.

The MAI in turns is due to not only the non-perfect orthogonality of the spreading sequences, but also the multipath effect. The multipath structure of the channel also causes signal fading, and may result in important power imbalances between the arriving signals of different users. Moreover, CDMA systems are particularly susceptible to the near-far problem [1]. A near-far situation is one in which a user or a group of users closer to the base station are likely to be received with significantly more power than those close to the cell boundary. As a matter of fact, the near-far effect is due to both multipath fading and to signal power loss as a function of distance from the base station. In this thesis, to mitigate such phenomena, we utilize space-time coding as a space-time processing technique that is well known to combat multipath fading, along with multiuser detection to combat MAI.

1.2 Motivation and Objective

Among the spread-spectrum techniques, the most popular one is Direct-Sequence CDMA (DS-CDMA) where each active user's data is modulated (multiplied) by a unique signature waveform. When the signature waveforms are not orthogonal, each user suffers from MAI emanating from the other active users.

Given the fact that Space-Time Codes (STCs) were initially designed for quasi-static fading channels, where the time variations of the channel are fixed within a frame and vary independently from one to another, no attempt was made to exploit the time diversity introduced by the channel. Recently, Firmanto *et al.* [2] have proposed a space-time trellis code (STTC) for fast-fading channels where the fading coefficients change independently from one symbol to another. The proposed STTC makes use of an exhaustive search to find codes that satisfy Tarokh *et al.* [3] design guidelines. Motivated by [2], we introduce a modified space-time transmit diversity scheme suitable for DS-CDMA systems over fast-fading channels. The proposed coding scheme is simple to implement, and adds minimal computational complexity to the original space-time block codes (STBC) in [4], [5]. In fact if the channel is slowly-fading, we show that the proposed transmit diversity scheme reduces to that of conventional transmit diversity schemes (for CDMA systems). We focus on the uplink scenario, where we use orthogonal codes to spread the transmitted signals according to a specified scheme and before transmitting them from the different antennas. As it will be shown, the proposed code design satisfies the orthogonality

condition required for efficient decoding operation. The proposed scheme in its beginning employs a STBC matrix that achieves its orthogonality condition using two orthogonal codes per user. The main objective of this thesis is to design a STC scheme for fast-fading channels that can improve the BER performance and at the same time, provide the full-promised diversity gain.

1.3 Thesis Contributions

In the light of the above mentioned objectives, the contribution of this thesis can be summarized as follows:

- We present a new space-time transmission scheme for a DS-CDMA system over fast-fading channels, and define the appropriate combining scheme.
- For the multiuser scenario, we analyze the performance of the proposed scheme when using the centralized MMSE, adaptive MMSE, decorrelator based receivers, where we obtain the centralized MMSE for this scheme. We show that even when the orthogonality condition is destroyed, using the adaptive MMSE multiuser detector offers only a small SNR degradation compared to the centralized MMSE, while the diversity order will be maintained.
- For the single-user case, and using orthogonal signature waveforms we conduct performance analysis, where we show that the probability of error has a a linear inverse relationship with the average SNR per channel.

- The study of the performance analysis of the proposed scheme for a DS-CDMA system with a decorrelator based multiuser receiver is studied for both fast and slow-fading channels. In this study, an upper bound that characterizes the degradation in BER for different system loads is defined.

The contributions of this thesis have resulted in three referred conference papers: [37], [40] and [45].

1.4 Thesis Outline

The thesis is organized as follows: In Chapter 2, we provide an overview of multiuser detection, where a description of a DS-CDMA multiuser system is given. We review and compare several multiuser detectors including the conventional and optimum multiuser detectors. Then we consider linear suboptimal detectors, where we discuss the advantages and disadvantages of each multiuser detector.

Chapter 3 introduces the proposed space-time spreading scheme for DS-CDMA systems designed for fast-fading channels. We provide the single and multiuser system models and the appropriate combining schemes used to recover the transmitted symbols. Then, we show that using orthogonal spreading codes one can achieve a two-fold of the diversity order obtained using existing space-time spreading schemes. We also show that even if the orthogonality condition is not satisfied (due to signal correlation between users and among themselves), one can still achieve the same

diversity order as the orthogonal case using an adaptive MMSE receiver. Furthermore, closed form expressions for the bit error probability of the single and multiuser systems are obtained.

In chapter 4 we study the performance of the proposed space-time spreading scheme over slow-fading channels with a decorrelator based receiver. We derived a closed form expression for the bit error rate, where we show that the full diversity order is maintained regardless of the number of active users and only an SNR loss is incurred. Using our theoretical results, we show that the loss in SNR from the single-user bound is upper bounded by $10\log(C/2)$ where (C) represents the sum of the two consecutive diagonal elements of the inverse of the cross-correlation matrix for the user under consideration.

Chapter 5 provides a brief summary of the accomplished work throughout this thesis with important conclusions. Some future suggestions are also made to extend the research in this area.

Chapter 2

Multiuser Detection and Space-Time Coding

Many advanced signal processing techniques have been proposed to combat multiple access interference and multipath channel distortion, and these techniques fall largely into two categories: multiuser detection [6] and space-time processing [7].

It has been well established that multiuser detection techniques can substantially enhance the receiver performance and increase the capacity of CDMA communication systems. Multiuser detection techniques exploit the underlying structure induced by the spreading waveforms of the DS-CDMA signals to jointly reduce the effect of interference. Various linear and nonlinear multiuser detectors have been developed over the past decade [6].

On the other hand, multi-antenna systems are well known as an effective technique to combat fading and to reduce the interference from interfering signals. Diversity techniques assume rich scattering where the signal arrives over several paths, and in order to achieve the maximum diversity it is necessary that fading signals at different antennas are uncorrelated or slightly correlated. Hence the probability that all paths are in deep fade at the same time is significantly smaller than that of a single transmission path. Multi-input multi-output systems or MIMO systems allow the receiver to see independent versions of the transmitted information which yields to spatial diversity and/or coding gain compared to single antenna systems. One approach that uses multiple transmit antennas and, if possible, multiple receive antennas to provide reliable and high data communication is space-time coding (STC) [3], [4].

In what follows we discuss briefly previous works in these areas. An outline of this chapter is as follows. In Section 2.1 we present the signal model for a DS-CDMA multiuser system. Then throughout this section we review different multiuser detectors, including the optimal, the decorrelator, the MMSE and the adaptive MMSE multiuser detectors. Section 2.2 gives a brief overview of space-time codes and MIMO Systems. The two most common signal processing space-time techniques: STBCs and STTCs are also discussed. Finally, Section 2.3 concludes this chapter.

2.1 Multiuser Detection

Multiuser Detection (MUD) is a technique that can be employed to improve the capacity and coverage in CDMA systems (Figure 2.1). In theory, MUD can provide an improvement in capacity in additive white Gaussian noise channels [6]. It has been shown in [6] that MUD is able to exploit the structure contained in a multi-access interference signal and in that way can be near-far resistant.

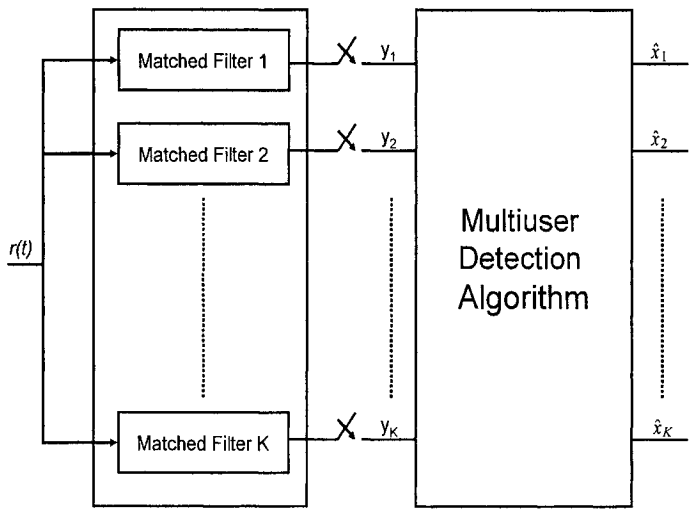

Figure 2.1: The concept of multiuser detection.

Research in the area of multiuser detection started in the late 1980s. In early stages, optimal solutions with best possible performance in Gaussian noise channels were investigated and developed. Unfortunately, the complexity of these solutions increases exponentially with the number of users, which is not suitable for practical applications. This problem has been tackled subsequently and resulted in less complex suboptimal multiuser detection algorithms such as the decorrelating detector,

the MMSE detector, and subtractive interference cancellation detectors [6].

2.1.1 Multiuser Signal Model

We consider a synchronous DS-CDMA system, where all users share the same bandwidth. The signaling interval of each symbol is T seconds, and the transmitted symbols take the values {+1, -1}. The received baseband signal in a single-path BPSK system for user k is given by

$$r_k(t) = \sum_{i=-\infty}^{\infty} A_k e^{j\theta_k} x_k(i) s_k(t - iT) \tag{2.1}$$

where $x_k(i)$ is the ith time-independent transmitted symbol by the kth user. A_k and θ_k are the signal amplitude and phase shift of user k, respectively. $s_k(t)$ is the kth user signature waveform assumed to have unit energy, where this spreading waveform can be written as

$$s_k(t) = \sum_{i=0}^{N-1} p_k[i] \Psi(t - iT_c) \tag{2.2}$$

with $\Psi(t)$ is the chip pulse shape, T_c is the chip duration, $N = T/T_c$ is the processing gain and $p_k[i] \in \{\pm 1/\sqrt{N}\}$, $i = 0, \ldots, N-1$, is the real-valued spreading sequence. In the remainder of this thesis we assume $\Psi(t)$ to be a square pulse on the interval $[0, T_c)$.

At the receiver side the received baseband signal is the noisy sum of all users'

signals. Considering a K-user system, the received multiuser signal is given by

$$r(t) = \sum_{k=1}^{K} \sum_{i=-\infty}^{\infty} A_k x_k(i) s_k(t - iT) + n(t) \tag{2.3}$$

where $n(t)$ is the complex additive white Gaussian noise with variance σ_n^2 per dimension. The received signal in (2.3) is sampled at the output of the chip matched filter. It is more convenient to express (2.3) in a vector form according to

$$\mathbf{r}=\mathbf{SAx}+\mathbf{n} \tag{2.4}$$

where $\mathbf{S} = [s_1, s_2, \ldots, s_k]$ and s_k is the column vector of spreading sequences for user k, $\mathbf{A}$ =diag$[A_1, A_2, \ldots, A_k]$, $\mathbf{x}$ =diag$[x_1, x_2, \ldots, x_k]^T$ is the symbol vector where the superscript "T" denotes matrix transpose, and $\mathbf{n}$ is the complex channel vector with covariance $\sigma_n^2\mathbf{I}$ where $\mathbf{I}$ is $K \times K$ diagonal matrix. It is worth to mention that we consider throughout this dissertation that some parameters are perfectly known, including amplitudes, phases and delays of the received signals.

2.1.2 Spreading Codes

In chapter 3 and 4, we have chosen a set of 32 Gold sequences that offer good cross-correlations [8]. Each of these sequences has a length 31 chips, where we assign two spreading codes for each user as the proposed space-time scheme dictates in the following chapters.

In the following we briefly review several previously proposed multiuser detectors of interest. Before doing so, we begin our discussion with the simplest detector, namely, the conventional detector.

2.1.3 Conventional Detector

Multiuser detectors commonly have a front-end whose objective is to obtain a discrete-time process from the continuous-time waveform in (2.3). Continuous to discrete time conversion is achieved by conventional sampling, or more generally, by the correlation of $r(t)$ with deterministic signals. Therefore, the first step in multiuser detection is to pass the received signal $r(t)$ through a bank of matched filters [8] (or correlators). The conventional detector corresponds to a bank of K matched filters, where each filter is matched to the signature of the desired user, and followed by a sampler as shown in Figure 2.2.

The performance of this detector depends on the properties of the correlation between codes. For synchronous CDMA, the output of the kth matched filter at the sampling time is given by

$$\begin{aligned} y_k &= \int_0^T r(t)s_k(t)dt \\ &= \int_0^T s_k(t)\left[\sum_{j=1}^{K} A_j x_j s_j(t) + n(t)\right] dt \\ &= A_k x_k + \sum_{j=1, j\neq k}^{K} A_j x_j R_{k,j} + \int_0^T s_k(t)n(t)dt \end{aligned} \tag{2.5}$$

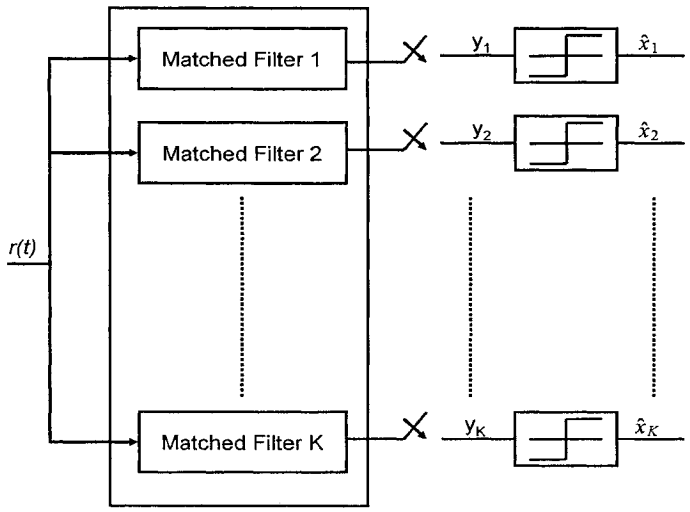

Figure 2.2: Block diagram of the conventional detector.

where

$$R_{k,j} = \int_0^T s_k(t)s_j(t)dt \tag{2.6}$$

is the cross-correlation between the spreading codes assigned to user k and user j. Note that y_k consists of three terms. The first term is the desired user's information, the second term is the result of the multiple access interference, and the last term is due to the noise. It is convenient to introduce the matrix-vector notation of (2.5) to describe the output of the conventional detector as follows

$$\mathbf{y}=\mathbf{RAx}+\mathbf{n} \tag{2.7}$$

where $\mathbf{R}$ is the $K \times K$ cross-correlation matrix with elements $R_{k,j}$, $\mathbf{y} = [y_1, y_2, \ldots, y_K]^T$,

and $\mathbf{n}$ is zero-Gaussian random vector with covariance matrix equal to

$$E[\mathbf{n}\mathbf{n}^T] = \sigma_n^2 \mathbf{R}. \tag{2.8}$$

Here, each code waveform is regenerated and correlated with the received signal in a separate detector branch. The outputs of the correlators or matched filters are sampled at the bit times, which yields "soft" estimate of the transmitted data. The final hard data decisions are made according to the signs of the soft estimates according to

$$\hat{x}_k = sgn(y_k). \tag{2.9}$$

Since the conventional detector ignores the MAI, thus its existence has a significant impact on the capacity and performance of conventional DS-CDMA systems.

2.1.4 Optimum Detector

The optimum multiuser detector shown in Figure 2.3, proposed by verdú in [9], is based on the Maximum-Likelihood (ML) detection. This ML detector selects the set of symbols corresponding to the signal among the possible ones which resembles most closely the received signal.

The optimum multiuser detector according to [9] can be expressed mathematically as

$$\hat{\mathbf{x}} = \arg \max_{\mathbf{x} \in \{-1,+1\}^K} \left\| r(t) - \sum_{j=1}^{K} A_j x_j s_j(t) \right\|. \tag{2.10}$$

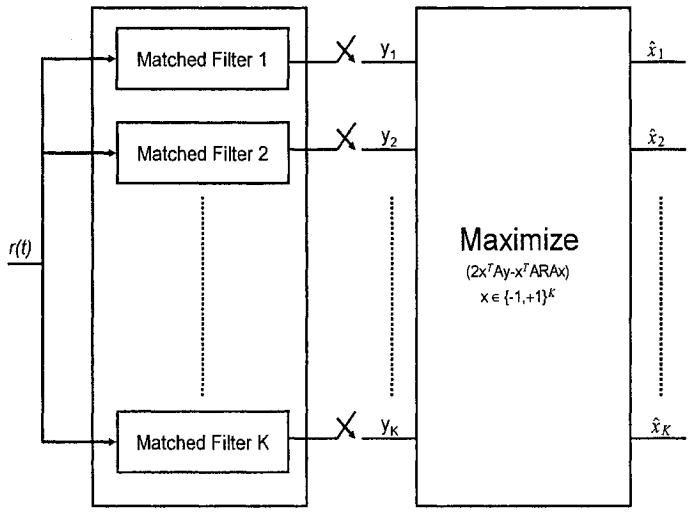

Figure 2.3: Block diagram of the optimum multiuser detector.

For a synchronous CDMA system, (2.10) may be written as

$$\begin{aligned}\hat{\mathbf{x}} &= \arg \max_{\mathbf{x}\in\{-1,+1\}^K} \int_0^T \left[r(t) - \sum_{j=1}^{K} A_j x_j s_j(t) \right]^2 dt \\ &= \arg \min_{\mathbf{x}\in\{-1,+1\}^K} \int_0^T r^2(t)dt - 2\sum_{j=1}^{K} A_j x_j \int_0^T r(t)s_j(t)dt \\ &+ \sum_{u=1}^{K}\sum_{j=1}^{K} A_u x_u A_j x_j \int_0^T s_u(t)s_j(t)dt \end{aligned} \tag{2.11}$$

or equivalently in matrix notation as

$$\hat{\mathbf{x}} = \arg \max_{\mathbf{x}\in\{-1,+1\}^K} \left(2\mathbf{x}^T\mathbf{A}\mathbf{y} - \mathbf{x}^T\mathbf{A}\mathbf{R}\mathbf{A}\mathbf{x}\right). \tag{2.12}$$

This kind of multiuser detectors provides the most reliable outputs and rejects the effect of MAI. Therefore, its performance is superior to all other detectors. In

spite of its superior performance, this ML detector as can be seen from (2.12), requires an exhaustive search over 2^K possible combinations of the vector $\mathbf{x}$ [10]. Hence, when the number of active users is large, the ML turns out to be too complex to implement. As a result, in what follows we discuss some suboptimum multiuser detectors that are less complex while offering a reasonable performance compared to the optimum multiuser detector.

2.1.5 Decorrelator Detector

As a linear mapper, the decorrelator detector applies the inverse of the cross-correlation matrix ($\mathbf{R}^{-1}$) to the conventional detector output in an attempt to cancel interference. Figure 2.4 shows the block diagram of a system that employs such a detector.

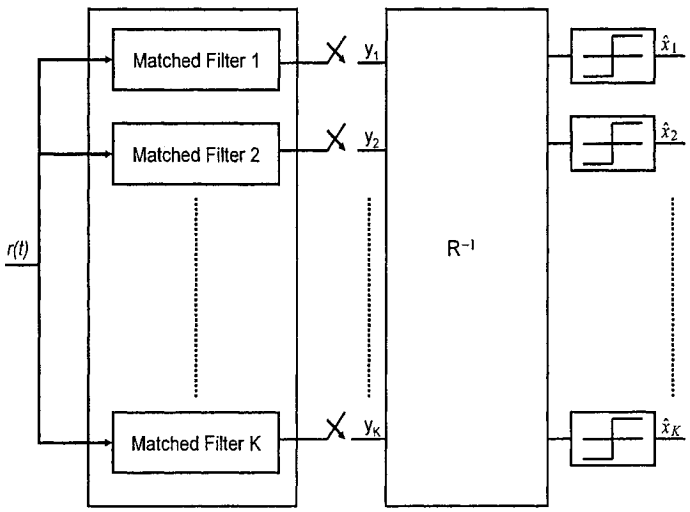

Figure 2.4: Block diagram of the Decorrelator multiuser detector.

The output of this detector using (2.7) is given by

$$\hat{\mathbf{y}} = \mathbf{R}^{-1}\mathbf{y} = \mathbf{A}\mathbf{x} + \mathbf{R}^{-1}\mathbf{n} \tag{2.13}$$

and the decision

$$\hat{\mathbf{x}} = sgn(\hat{\mathbf{y}}). \tag{2.14}$$

Thus, this approach, first proposed in [11, 12] and analyzed extensively by Lupas and Verdú in [13, 14], eliminates the MAI completely in a manner analogous to the zero-forcing equalizer [8]. The error rate of the decorrelator detector for user k is found in [6] to be

$$P_k = Q\left(\frac{A_k}{\sigma_n\sqrt{(\mathbf{R}^{-1})_{k,k}}}\right) \tag{2.15}$$

where the Q-function is defined by $Q(x) = \int_x^\infty \frac{1}{\sqrt{2\pi}} exp(-\frac{v^2}{2})dv$ and $(\mathbf{R}^{-1})_{k,k}$ represents the element k,k of the inverse of the cross-correlation matrix. (2.15) shows that the performance of the decorrelator detector degrades as the cross-correlations between users increase. The decorrelator detector offers many advantages, among these:

- It does not require the knowledge of the users' signal energies, hence its performance is independent of the energies of the interfering users, or in other words it is near-far resistant.

- It provides significant performance gain over the conventional detector.

- The computational complexity of the decorrelator is much less than the optimum multiuser detector. Excluding the costs of computation of the inverse of the cross-correlation matrix, its complexity is linear in the number of users.

The disadvantages of this detector can be summarized as follows:

- As it is seen from (2.13), this detector enhances the background noise at its output. It has been shown in [15] that the output noise of the decorrelator detector is always equal to or greater than the output noise of the conventional detector.

- The computation of the inverse of the cross-correlation matrix $\mathbf{R}$ is difficult to perform in real-time, particularly in an asynchronous environment.

- In some special cases, $\mathbf{R}^{-1}$ does not exist [6].

In spite of these disadvantages, the decorrelator detector provides a good performance which in most cases is close to the optimum multiuser detector.

2.1.6 MMSE Detector

Based on the MMSE criterion, the MMSE detector implements linear mapping to minimize the MSE between the actual data and the soft output of the MMSE detector. The MMSE detector was studied for both synchronous and asynchronous channels in [16], [17] and [18]. The linear mapping of the MMSE detector shown in

Figure 2.5 is given by [16]

$$\mathbf{W}_{MMSE} = \left[\mathbf{R} + \sigma_n^2 \mathbf{A}^{-2}\right]^{-1}. \tag{2.16}$$

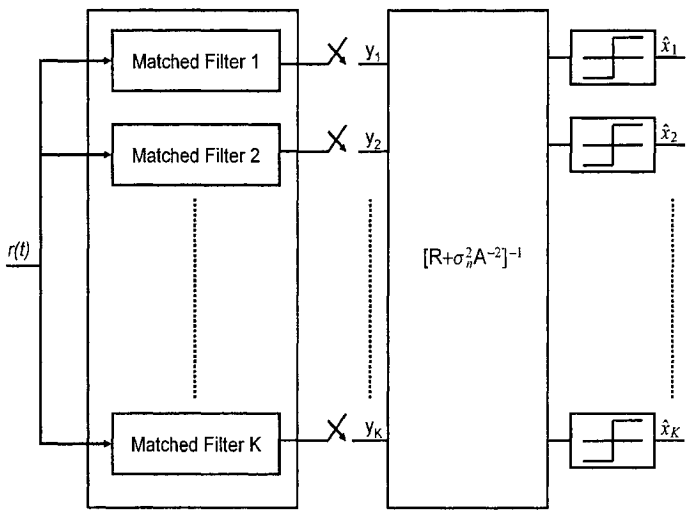

Figure 2.5: Block diagram of the MMSE multiuser detector.

Hence, the estimate of the transmitted symbol at the output of the MMSE detector follows simply as

$$\hat{\mathbf{y}} = \mathbf{W}_{MMSE}\mathbf{y}. \tag{2.17}$$

As can be seen, the MMSE detector implements a partial or modified inverse of the cross-correlation matrix. Because it takes the background noise into account, the MMSE detector generally provides better probability of error performance than the decorrelating detector. However, from (2.16), as the background noise goes to zero, the MMSE detector converges in performance to the decorrelating detector. The

operation of the MMSE detector can be viewed as offering a balance between interference cancellation and noise enhancement. Compared to the decorrelator detector, an important feature of the MMSE is that it can be implemented adaptively, as in [19]-[21], which eliminates the need to know the signature sequences, time and amplitudes. Another advantage of the MMSE detector is that the linear transformation $\mathbf{W}_{MMSE}$ always exists even when $\mathbf{R}^{-1}$ is singular.

A main disadvantage of the MMSE detector is that unlike the decorrelator detector, it requires estimation of the received signal amplitudes. Another disadvantage is that its performance depends on the powers of the interfering users. Therefore, there is some loss in resistance to the near-far problem as compared to the decorrelating detector.

2.1.7 Adaptive MMSE Detector

The adaptive receivers applying interference suppression mechanisms have been proposed in [19], [22], [23]. As noted earlier, the MMSE detector requires an exact knowledge of the signature sequences and that of the amplitude of the received signals of all the users.

In [22], an adaptive MMSE multiuser detector was proposed, which replaces the need of a priori knowledge of all other user signature waveforms by using a training data sequence for each user in the system. The operation of the adaptive MMSE detector requires each user to first transmit a training sequence that is used

by the receiver for initial adaptation. After the training phase ends, adaptation for actual data transmission is realized by making use of the transmitted data. However, at any time when there is a dramatic change in the interfering environment, a new training sequence is usually sent. The frequent use of training sequences is certainly a waste of channel bandwidth. In practice, it is common to perform fine adjustments of the linear transformation (once the adaptive algorithm has converged and the transmission of the training sequence is over) by letting the adaptive algorithm run with the decision made by the detector in lieu of the true transmitted data. This type of operation is usually referred to as decision-directed.

As shown in [16], [19], [20], [22], [24] and [25] the adaptive MMSE receiver can be implemented as an adaptive tapped-delay line filter blindly or with the help of training sequence (Figure 2.6). The computational complexity involved in adaptive MMSE detectors is found to be comparable with that of the conventional matched filter detector [16]. However, adaptive MMSE detectors usually offer significant improvement in performance. Tracking speed and computational complexity are two primary concerns in designing adaptive MMSE multiuser detectors. In order to improve the tracking speed in a time varying wireless communication environment and to reduce the length of training sequence for tracking, fast converging adaptive MMSE detectors with low computational complexity are required. Some algorithms with low complexity, e.g., the least-mean-square (LMS) algorithm, have been proposed for adaptive MMSE multiuser detection [20].

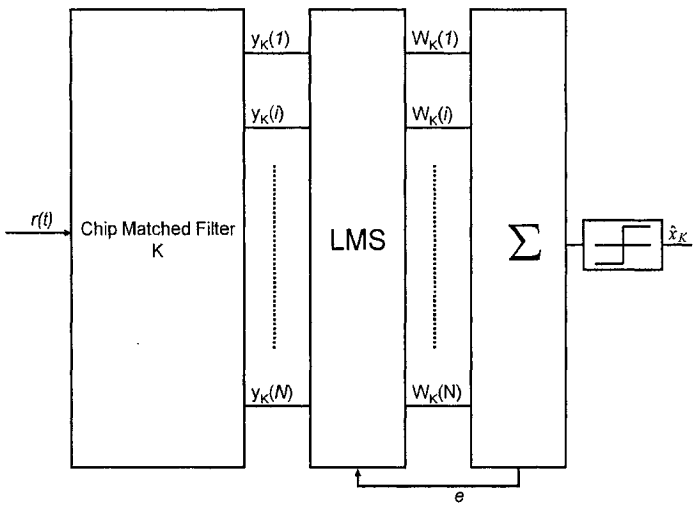

Figure 2.6: LMS based adaptive MMSE multiuser detector.

2.2 Space-Time Codes

Systems which use multiple transmit and receive antennas for communication over a wireless channel are usually called Multiple-input multiple-output (MIMO) systems. This section gives an introduction to MIMO systems or more specifically, space-time coding, a technique used to transmit user data from multiple antennas.

2.2.1 Multiple-Input Multiple-Output (MIMO) Systems

To effectively evaluate the performance of a MIMO transmission scheme, models which account for all the major effects of wireless channel on various signals are required. The most commonly used channel model for MIMO systems is the quasi-static flat Rayleigh fading model. This was employed in [3], [4] and [26] where novel signal processing schemes for MIMO systems were introduced. The simplicity of this

channel model made the performance analysis of these schemes less complicated, allowing to place more emphasis on introducing the transmit and receive signal processing algorithms. Fundamental information theoretic results on capacity of MIMO channels [27] and transmit diversity techniques also employ a similar fading model. The basic assumptions behind the quasi-static flat Rayleigh fading channel are

- A large number of scatterers are present in the wireless channel so that the signal at any receive antenna of the MIMO system is the sum of several multipath components. In this case the distribution of the received signal at each antenna will be complex Gaussian. The amplitude of such complex Gaussian distributed signals is Rayleigh distributed.

- The channel delay spread, which is a measure of the difference in the time of arrival of various multipath components at the receiver antenna, is less than the symbol rate. This assumption guarantees flat fading.

- The channel characteristics remain constant at least for the period of transmission of an entire frame. This assumption accounts for quasi-static fading.

Using all these assumptions, the quasi-static flat Rayleigh fading MIMO channel for a system with n transmit and m receive antennas can be represented as

$$\mathbf{H} = \begin{bmatrix} h_{11} & h_{12} & \dots & h_{1n} \\ h_{21} & h_{22} & \dots & h_{2n} \\ \vdots & \vdots & \ddots & \vdots \\ h_{m1} & h_{m2} & \dots & h_{mn} \end{bmatrix} \tag{2.18}$$

where h_{ij} is the path gain between receive antennas i and transmit antenna j. The path gains are usually modelled as zero mean complex Gaussian random variables with variance 0.5 per dimension.

2.2.2 Diversity Techniques

Let us consider a system with BPSK modulation transmitting over a fading channel with Gaussian noise. The complex channel coefficient is denoted by h and its magnitude is denoted by α. It is assumed that the phase of fading coefficients is perfectly known at the receiver (i.e. coherent detection). The conditional error rate of BPSK as a function of channel coefficient over frequency non-selective, slowly fading channel is given by [8]

$$P_b(\alpha) = Q(\sqrt{2\gamma}) \tag{2.19}$$

where $\gamma = \frac{\alpha^2 E_b}{No}$ is the received SNR. To find the average error rate, we must integrate over the distribution of the fading coefficients. Assuming Rayleigh fading, this integration leads to [8]

$$P_b = \frac{1}{2}\left(1 - \sqrt{\frac{\overline{\gamma}}{1+\overline{\gamma}}}\right) \tag{2.20}$$

where $\overline{\gamma} = \frac{E_b}{No} E(\alpha^2)$ is the average SNR. At high SNR, this error probability can be approximated as

$$P_b \approx \frac{1}{4\overline{\gamma}}. \tag{2.21}$$

Note that the error rate decreases inversely with SNR. Compare this to the error rate of BPSK in non-fading (AWGN) channel [8]

$$P_b = Q\left(\sqrt{\frac{2E_b}{No}}\right) \tag{2.22}$$

which decreases exponentially with SNR. This means that on a fading channel the transmitter should transmit with more power to achieve a low probability of error.

As mentioned in the first chapter, diversity techniques are very effective against fading channels. If we can supply several replicas of the transmitted signal to the receiver, it is unlikely that all of them will undergo deep fade simultaneously. If we have supplied L independently faded replicas of transmitted signal to the receiver, and p is the probability that any one replica will undergo deep fading, p^L is the probability that all the L replicas will undergo deep fading. There are several types of diversity techniques: frequency diversity, polarization diversity, time diversity,

and spatial diversity.

Traditionally, there is only single transmit antenna and multiple receive antennas. This technique is referred to as receive diversity. The receiver can use one of three techniques to improve the quality of the received signal

1. Selection: select the received signal with largest received power.

2. Switching: choose alternate antennas if the received power falls below a threshold level.

3. Maximal Ratio Combining (MRC): linearly combine a weighted replica of all received signals.

In the method of MRC, it is assumed that the receiver has perfect channel state information. If the transmitted signal at time t is $s(t)$, then the received signal at receiver i is given by

$$r_i(t) = h_i(t)s(t) + n_i(t) \tag{2.23}$$

where $n_i(t)$ is complex noise variable. Assuming that this noise is Gaussian, the receiver combining scheme is

$$\hat{r}_i(t) = \sum_{i=1}^{m} h_i^* r_i(t) = s(t) \sum_{i=1}^{m} |h_i|^2 + \acute{n}_i(t). \tag{2.24}$$

This detected symbol is then passed through a maximum-likelihood detector to produce the estimate of the transmitted signal $\hat{s}(t)$. MRC provides full diversity,

but due to channel estimation the complexity is high.

2.2.3 Space-Time Block Codes

The receive diversity scheme is not suitable for the downlink, as it is difficult and inconvenient to place multiple antennas on handsets. The multiple antenna burden is preferably placed at the base station. This is called transmit diversity. Transmit diversity has gained much attraction in the last decade [4, 26]. Unlike receive diversity, in transmit diversity, it is not possible to transmit the same signal from all antennas. If the same signal is transmitted from all antennas, at the receiver the copies of this signal add incoherently, and no diversity gain can be achieved. Thus in order for transmit diversity to work, one must find a transmission scheme where replicas of the signal combine coherently at the receiver.

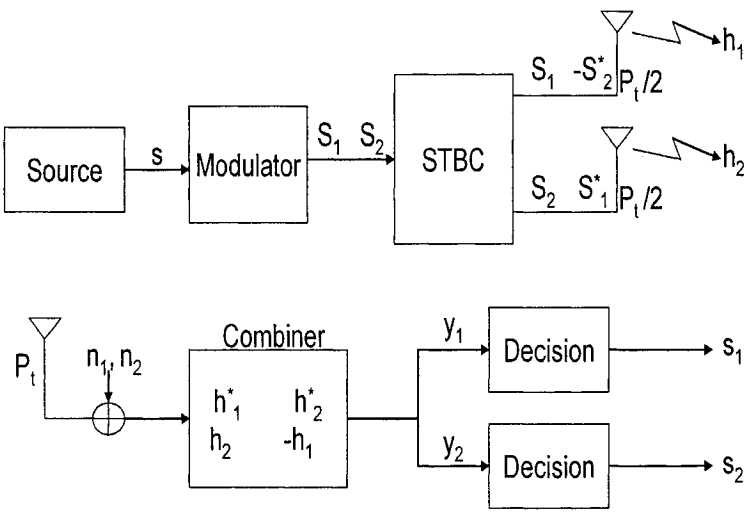

Figure 2.7: Transmitter and receiver structures for Alamouti's transmission scheme.

One of the simplest and most attractive transmit diversity schemes shown in Figure 2.7 which was proposed by Alamouti [4]

$$\Im = \begin{bmatrix} s_1 & s_2 \\ -s_2^* & s_1^* \end{bmatrix} \tag{2.25}$$

where * denotes complex conjugate operation, the rows denote time instances and the columns denote the corresponding transmitting antenna. Thus, at time $t = 1$, s_1 and s_2 will be transmitted from antennas 1 and 2 respectively, and at time $t = 2$, $-s_2^*$ and s_1^* will be transmitted from antennas 1 and 2 respectively. One can see that two symbols are transmitted over two time intervals. Hence the code is full rate. Assuming a single receiver, let h_1 and h_2 denote the channel coefficients for transmit antenna 1 and 2 respectively. The fading coefficients are assumed to be constant over two consecutive time slots, hence the received signal is

$$y_1 = h_1 x_1 + h_2 x_2 + n_1 \tag{2.26}$$

$$y_2 = -h_1 x_2^* + h_2 x_1^* + n_2. \tag{2.27}$$

Assuming perfect CSI, this can be maximum-likelihood (ML) decoded as

$$\hat{x}_1 = h_1^* y_1 + h_2 y_2^* = (|h_1|^2 + |h_2|^2) x_1 + n_1 \tag{2.28}$$

$$\hat{x}_2 = h_2^* y_1 - h_1 y_2^* = (|h_1|^2 + |h_2|^2) x_2 + n_2. \tag{2.29}$$

We observe from the above expression that by using two transmit and one receive antenna, the transmitted signals are multiplied by $|h_1|^2 + |h_2|^2$. Hence, if one of the paths is in deep fade, the other may still represent the true transmitted signal.

Tarokh *et al.* [26] extended the Alamouti's 2-transmit diversity scheme to more than two antennas. This new generalized space-time signaling scheme is known as space-time block codes (STBC). Later, Alamouti's scheme was generalized to a wireless system with n transmit and m receive antennas, hence the name STBC. Space-time block codes derive their name from the fact that the encoding is done in both space and time, and their encoder is defined simply by a matrix. A space-time block code is defined by the relationship between the k-tuple input signal x and the set of signals to be transmitted from n antenna over p time periods. Such a relation is given by $p \times n$ transmission matrix

$$\Im = \begin{bmatrix} s_{11} & s_{12} & \cdots & s_{1n} \\ s_{21} & s_{22} & \cdots & s_{2n} \\ \vdots & \vdots & \ddots & \vdots \\ s_{p1} & s_{p2} & \cdots & s_{pn} \end{bmatrix} \tag{2.30}$$

where s_{ij} are functions of k-tuple input sequence $x_1, x_2, \ldots, x_k$ and their complex conjugates. At time slot i, s_{ij} is transmitted from antenna j. Since k information bits are transmitted over p time intervals, the rate of the code is defined as $R = \frac{k}{p}$. At the receiver we can use arbitrary number of receive antennas. If $\Im\Im^H = \alpha\mathbf{I}$,

where $\alpha = \sum_{n=1}^{n} |s_n|^2$ and $\mathbf{I}$ is the identity matrix, the code is called orthogonal STBC. The orthogonal STBC assumes that the channel coefficients are constant over a period of n symbols, i.e.

$$h_{ij}(t) = h_{ij} \qquad t = 1, 2, \ldots, n. \tag{2.31}$$

This block fading assumption is required for simple linear decoding of OSTBC. OSTBC also assumes that the channel is frequency non-selective. If the channel is frequency selective, one can use orthogonal frequency division multiplexing (OFDM) to split the input bit stream into large number of low-rate streams transmitted over flat-fading channels. In our work, we only consider frequency non-selective channels.

At the receiver, the m receive antennas use maximum-likelihood (ML) decoding. In orthogonal STBC, the ML decoding is equivalent to maximum ratio combining (MRC). Assuming perfect channel state-information, the decoder at antenna j maximizes

$$\sum_{t=1}^{p} \sum_{j=1}^{n_R} |r_j^t - \sum_{i=1}^{n} h_{ij} x_j^t|^2. \tag{2.32}$$

Since the block coding requires only linear processing at the receiver, the decoding can be done efficiently. Space-time block codes can be constructed for any type of signal constellation and provide full diversity. However, only real constellations such as Pulse Amplitude (PAM) can give full rate for any number of antennas. For complex constellations such as Phase Shift Keying (PSK), full rate STBCs exist only

for n=2.

2.2.4 Space-Time Trellis Codes

Space-time trellis codes (STTCs), originally proposed by Tarokh *et al.* [3], incorporate jointly designed channel coding, modulation, transmit diversity and optional receive diversity. As the name suggests, the structure of space-time trellis code is given by a trellis. A trellis for 4-state QPSK STTC with two transmit antennas is given in Figure 2.8.

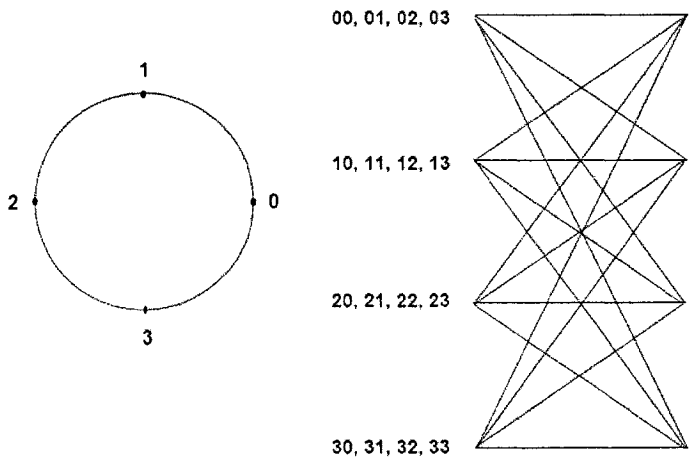

Figure 2.8: Tarokh's 4-state QPSK space-time trellis code [3].

Here the first QPSK symbol is transmitted from first antenna and the second QPSK symbol is transmitted from second antenna, at time instance t. Thus, at each time instance one information symbol is transmitted, and the rate is one.

The $m \times 1$ received signal is given by

$$\mathbf{y}^t = \mathbf{H}^t\mathbf{s}^t + \mathbf{n}^t \tag{2.33}$$

where $\mathbf{H}$=h_{ij}, $i = 1, \ldots, n$, $j = 1, \ldots, m$ is the channel coefficients matrix, and $s = [s_1, \ldots, s_n]^T$ is the transmitted data vector at time instance t. A codeword c is defined as

$$\mathbf{c} = \begin{bmatrix} c_1(1) & c_1(2) & \ldots & c_1(N) \\ c_2(1) & c_2(2) & \ldots & c_2(N) \\ \vdots & \vdots & \ddots & \vdots \\ c_n(1) & c_n(2) & \ldots & c_n(N) \end{bmatrix} \tag{2.34}$$

where an error event is given by $\mathbf{B}(\mathbf{c}, \mathbf{e}) = \mathbf{c} - \mathbf{e}$. The probability of erroneously decoding $\mathbf{e}$ when $\mathbf{c}$ was transmitted, called pairwise error probability (PEP), is given by [3]

$$P(c, e) \leq \left(\prod_{i=1}^{r} \lambda_i \right)^{-m} \left(\frac{E_s}{4No} \right)^{-rm} \tag{2.35}$$

where r is the rank of $\mathbf{A}(\mathbf{c}, \mathbf{e}) = \mathbf{B}(\mathbf{c}, \mathbf{e})\mathbf{B}^H(\mathbf{c}, \mathbf{e})$ and λ are the nonzero eigenvalues of $\mathbf{A}(\mathbf{c}, \mathbf{e})$. From (3.21), the design criteria can be given as

1. Rank criterion: To achieve maximum possible diversity, $n \times m$, matrix $\mathbf{A}(\mathbf{c}, \mathbf{e})$ should be full rank for all the codewords.

2. Determinant criterion: To maximize the coding gain, minimum determinant of $\mathbf{A}(\mathbf{c}, \mathbf{e})$ should be maximized over all codewords.

2.3 Conclusion

In this chapter, we presented the signal model of a typical DS-CDMA system, and provided a general idea of the concept of multiuser detection. Then, a comprehensive study of several multiuser detectors was given, where we introduced their advantages and disadvantages. We demonstrated that the optimum multiuser detector provides large gains compared to the conventional detector, but due to its complexity, its implementation is considered impractical. Hence, the decorrelator and MMSE multiuser detectors were introduced as a tradeoff between performance and computational complexity. The decorrelator detector can operate without knowledge of the received amplitudes, while the MMSE detector, which offers better performance, requires the knowledge of received powers. In real life scenarios, this could be to much to ask for, therefore adaptive MMSE implementations were proposed. Furthermore, we reviewed briefly the concepts of space-time codes and MIMO systems, and demonstrated its major role in multipath fading mitigation. We reviewed later STBCs and STTCs as two examples of signal processing over fading channels. Orthogonal STBCs provide an easy and efficient method to utilize the channel multipath components to achieve higher gains. STTCs, on the other hand, achieves better performance with coding gains.

Chapter 3

Space-Time Spreading over Fast-Fading Channels

According to the discussion in the previous chapter, it is evident that DS-CDMA systems suffer from two major drawbacks: MAI and multipath fading. To overcome these drawbacks, we introduced multiuser detection and space-time coding. The study of the optimum detector showed that despite its superior performance over the conventional detector, its complexity makes its implementation practically impossible. Therefore, suboptimum multiuser detectors were proposed to alleviate the complexity problem and to offer a tradeoff between performance and complexity. We showed that although STBCs have simple structure and decoding techniques, they suffer from significant performance degradation compared to STTCs since they don't

offer coding gains. In this chapter we introduce a space-time spreading transmission scheme for DS-CDMA systems designed for fast-fading channels. This scheme utilizes the full diversity promised by the channel, and hence provide high diversity gains compared to existing space-time block codes.

The rest of this chapter is organized as follows. In Section 3.1 previous work in this research area is summarized and the contribution of this chapter is reviewed. Section 3.2 introduces the proposed scheme, while Section 3.3 presents the single-user system model and the probability of error for the single-user case. The proposed adaptive MMSE receiver for the underlying scheme is given in Section 3.4. Section 3.5 provides the multiuser system model for the proposed scheme. The centralized MMSE mapping is then developed in Section 3.6. We obtain the probability of bit error for a receiver that employs the decorrelator MUD in Section 3.7. The simulation and analytical results are presented and compared in Section 3.8 for both the single and multiuser environments. Finally, Section 3.9 concludes this chapter and summarizes the obtained results.

3.1 Introduction

To reduce the large complexity of STTCs, Alamouti in [4] introduced a very simple, yet efficient, coding scheme that uses two transmit antennas at the base station (BS) and one receive antenna at the other end of the down-link. A simple decoding algorithm was introduced for this scheme, which can be extended to arbitrary number of

receive antennas. Motivated by the simplicity of Alamouti's scheme, Tarokh, *et al.* [26] generalized that scheme to an arbitrary number of transmit antennas, resulting in the so called space-time block codes. It is known that, for the same number of transmit and receive antennas, both STTC and STBC normally achieve the same spatial diversity. However, despite the low complexity they offer, STBCs do not offer any coding gain, unlike the case of STTCs [28]-[29]. Therefore, STBC needs to be combined with a channel coding scheme in order to provide such coding gains [30]-[34].

Given the fact that STCs were initially designed for quasi-static fading channels, where the time variations of the channel are fixed within a frame and vary independently from one to another, no attempt was made to exploit the time diversity introduced by the channel. Firmanto *et al.* [2] proposed a STTC for fast-fading channels where the fading coefficients change independently from one symbol-to-another. The proposed STTC makes use of an exhaustive search to find codes that satisfy Tarokh *et al.* [3] design guidelines.

Jayaweera and Poor in [35] (and references therein) realized the importance of space-time coding in multiuser CDMA systems over fading channels. In their work, they proposed a turbo multiuser receiver for space-time coded systems. Motivated by their work, in [36], a space-time block coding scheme that achieves its orthogonality using four codes per user was introduced. Later, in [37], we introduced a transmit diversity scheme based on space-time spreading and suited for CDMA systems over

fast-fading channels. The scheme in [37] was shown to utilize both the spatial and temporal diversities at the transmitter side to enhance the reception quality of the transmitted signal. Moreover, it was shown in [37] that, if the channel is slowly fading, the proposed transmit diversity scheme reduces to that of conventional schemes (for CDMA systems) [5].

3.2 Proposed Space-Time Scheme

In this section, we propose a simple space-time spreading scheme for CDMA systems over Rayleigh fast-fading channels. The proposed transmit diversity scheme is based on $N = 2$ transmit and M receive antennas and is designed for fast-fading channels. In this we employ orthogonal spreading codes to exploit the time diversity introduced by the channel, and hence a two-fold of the diversity order obtained using existing space-time spreading schemes is achieved. Then, we examine the effect of using nonorthogonal spreading codes on the receiver performance. Our results show that using a simple adaptive decoder, based on the MMSE criterion, the diversity order is still maintained and only a small loss in the signal-to noise ratio is incurred relative to the ideal case with orthogonal codes. For the single user case, and using orthogonal spreading codes, we develop the performance analysis for the underlying transmit diversity scheme over fast-fading channels. Further, we consider the case of nonorthogonal codes where we employ a linear MMSE multiuser detector as a suboptimum detector. The performance of the multiuser system is

examined for a moderate number of users, where we compare the performance of the MMSE multiuser detector with the simple adaptive MMSE combining scheme. In addition, we emphasize on finding a statistical semi-analytical model for the performance analysis of the multiuser system. Then, we prove the accuracy of this model by comparing the simulations with the semi-analytical results. Furthermore, we commence the mathematical analysis by finding the probability density function (pdf) for the signal-to-interference ratio (SIR) through the transformation of random variables. Moreover, we use numerical integration methods to check the validity of this pdf. We show that by averaging over this pdf, a closed form expression for the probability of error using the decorrelator multiuser detector can be obtained. Finally, using this expression we prove that the full diversity order is maintained as a linear inverse relationship with the average SNR per channel. We verify the accuracy of the expression by comparison with simulations for different number of users.

3.3 System Model

The system under consideration models an uplink of a wireless communication system that employs $N = 2$ antennas at the transmitter side and M antennas at the receiver side. Without loss of generality, we show in Figure 3.1 the case of two transmit and one receive antennas for this system. The channel is modelled as a flat

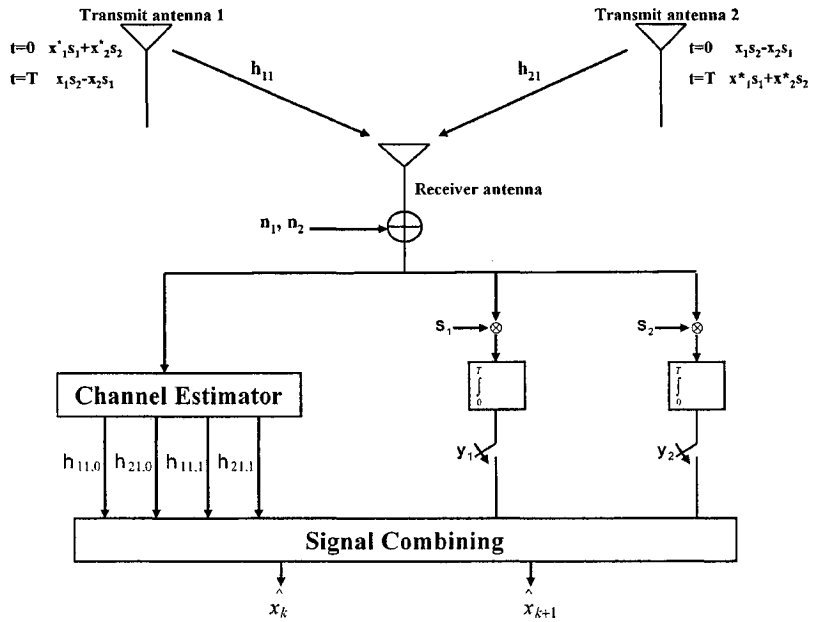

Figure 3.1: The proposed space-time spreading scheme for two transmit and one receive antenna.

fast-fading channel where the channel coefficients are considered to be fixed during one symbol interval and change independently from one symbol to another. A space-time spreading scheme that employs two codes per user, and hence reducing the effect of signal interference, is introduced.

3.3.1 Space-Time Spreading and Encoder Design

Following the system model in [37], and as shown in Figure 3.1, user data is transformed into an even and odd data streams, x_1, x_2, at the input of the space-time encoder. The encoder then performs signal spreading to the input parallel data

streams using two unique code sequences $s_i, i = 1, 2$ (i.e., known only to the desired user). Note that, here, we incorporated the signal spreading operation into the space-time encoder. After signal spreading, the encoder then forms a space-time code matrix given by

$$\begin{array}{lll} & \text{Tx Antenna (1)} & \text{Tx Antenna (2)} \\ t = 0, & x_1^* s_1 + x_2^* s_2 & x_1 s_2 - x_2 s_1 \\ t = T, & x_1 s_2 - x_2 s_1 & x_1^* s_1 + x_2^* s_2. \end{array} \tag{3.1}$$

The code sequences, s_1 and s_2, are given by

$$s_i(t) = \sum_{k=1}^{L-1} p_i[k] \Psi(t - kT_c) \tag{3.2}$$

where $\Psi(t)$ is the chip pulse shape, T_c is the chip duration, $L = T/T_c$ is the processing gain with T being the symbol period, and $p_i[k] \in \left\{\pm 1/\sqrt{L}\right\}$, $k = 0, ..., L-1$, is the real-valued spreading sequence. In the remainder of this work, we take $\Psi(t)$ to be a square pulse with the interval $[0, T_c)$. As seen from the code matrix in (3.1), the encoder produces codewords $x_1^* s_1 + x_2^* s_2$ and $x_1 s_2 - x_2 s_1$ to be transmitted from antenna 1 and 2, respectively, during the first transmission period. In the second transmission period, these codewords are switched with respect to the antenna order. It is important to mention that, in our development, we fix the total transmitted power to that of maximal-ratio combining (MRC) with the same number of

antennas (i.e., one transmit and two receive antennas).

Note that the proposed space-time spreading code still preserves the orthogonality condition [4]. That is, if

$$\mathbf{X}_1 = [\, x_1^* s_1 + x_2^* s_2, x_1 s_2 - x_2 s_1]$$

and

$$\mathbf{X}_2 = [x_1 s_2 - x_2 s_1, x_1^* s_1 + x_2^* s_2]$$

then, $\mathbf{X}_1.\mathbf{X}_2^H = 0$ where we assumed that the spreading codes are orthogonal and have unit energy ($\int_0^T \|s_k(t)\|^2\, dt = 1$).

3.3.2 Space-Time Spreading and Decoder Design

The receiver structure is shown schematically in Figure 3.1. Given the transmitted code matrix in (3.1), the received signal at the mth receive antenna can be written as

$$r_0^m = h_{1m,0}(x_1^* s_1 + x_2^* s_2) + h_{2m,0}(x_1 s_2 - x_2 s_1) + n_0^m \tag{3.3}$$

at time t, and as

$$r_1^m = h_{1m,1}(x_1 s_2 - x_2 s_1) + h_{2m,1}(x_1^* s_1 + x_2^* s_2) + n_1^m \tag{3.4}$$

at time $t+T$, where the noise n_0^m, n_1^m are modelled as independent samples of zero-mean complex Gaussian random variables, each with variance $\sigma_n^2 = N_0/2$ per dimension. In (3.3) and (3.4), the coefficients $h_{nm,j} = \alpha_{nm}e^{j\theta_{nm}}$ model the fading between the n^{th}, $n = 1, 2$, transmit and m^{th}, $m = 1, ..., M$ receive antenna at time j, $j = 0, 1$, and are assumed to be independent complex Gaussian random variables with variance 0.5 per dimension.

Before signal combining, the received signals in (3.3) and (3.4) are first applied to a bank of two matched filters where each filter is matched to one of the two assigned code sequences. The output of these filters, after sampling, is given in a vector form by

$$\mathbf{y}_0^m = \mathbf{X}_0\mathbf{h}_0^m + \mathbf{N}_0^m \tag{3.5}$$

at time t, and by

$$\mathbf{y}_1^m = \mathbf{X}_1\mathbf{h}_1^m + \mathbf{N}_1^m \tag{3.6}$$

at time $t+T$, where

$$\mathbf{y}_0^m = [y_{0,1}^m \quad y_{0,2}^m]^{\mathrm{T}}, \quad \mathbf{y}_1^m = [y_{1,1}^m \quad y_{1,2}^m]^{\mathrm{T}}, \tag{3.7}$$

$$\mathbf{X}_0 = \begin{bmatrix} x_1^* + x_2^*\rho_{12} & x_1\rho_{12} - x_2 \\ x_1^*\rho_{21} + x_2^* & x_1 - x_2\rho_{21} \end{bmatrix},$$

$$\mathbf{X}_1 = \begin{bmatrix} x_1^* + x_2^*\rho_{12} & x_1\rho_{12} - x_2 \\ x_1^*\rho_{21} + x_2^* & x_1 - x_2\rho_{21} \end{bmatrix}, \tag{3.8}$$

$$\mathbf{h}_0^m = \begin{bmatrix} h_{1m,0} \\ h_{2m,0} \end{bmatrix}, \quad \mathbf{h}_1^m = \begin{bmatrix} h_{2m,1} \\ h_{1m,1} \end{bmatrix}, \tag{3.9}$$

$$\mathbf{N}_0^m = [N_{0,1}^m \quad N_{0,2}^m]^{\mathrm{T}}, \ \mathbf{N}_1^m = [N_{1,1}^m \quad N_{1,2}^m]^{\mathrm{T}} \tag{3.10}$$

where $\mathbf{y}_0^m$ and $\mathbf{y}_1^m$ are (2×1) vectors with elements $y_{0,i}^m$, $y_{1,i}^m$, $i = 1, 2$, ρ_{ij} is the cross-correlation between the ith and jth spreading codes. The (2×1) vector $\mathbf{h}_j^m$ represents the channel coefficients with elements $h_{nm,j}$, $n = 1, 2$, $m = 1, ..., M$, $j = 0, 1$, while $\mathbf{N}_{0,i}^m$ and $\mathbf{N}_{1,i}^m$, $i = 1, 2$ are complex Gaussian random variables, each with variance $N_o/2$ per dimension. With perfect channel state information, the receiver performs signal combining on the output of the matched filter bank according to

$$\widehat{x}_1 = \sum_{m=1}^{M} h_{1m,0} y_{0,1}^{m*} + h_{2m,0}^* y_{0,2}^m + h_{1m,1}^* y_{1,2}^m + h_{2m,1} y_{1,1}^{m*} \tag{3.11}$$

$$\widehat{x}_2 = \sum_{m=1}^{M} h_{1m,0} y_{0,2}^{m*} - h_{2m,0}^* y_{0,1}^m - h_{1m,1}^* y_{1,1}^m + h_{2m,1} y_{1,2}^{m*}. \tag{3.12}$$

Assuming orthogonal spreading waveforms, the data estimates in (3.11) and (3.12)

are given by

$$\widehat{x}_1 = \sum_{m=1}^{M} \left(|h_{1m,0}|^2 + |h_{2m,0}|^2 + |h_{1m,1}|^2 + |h_{2m,1}|^2 \right) x_1 + h_{1m,0} n_{0,1}^{m*} + h_{2m,0}^{*} n_{0,2}^{m} + h_{1m,1}^{*} n_{1,2}^{m} + h_{2m,1} n_{1,1}^{m*} \tag{3.13}$$

and

$$\widehat{x}_2 = \sum_{m=1}^{M} \left(|h_{1m,0}|^2 + |h_{2m,0}|^2 + |h_{1m,1}|^2 + |h_{2m,1}|^2 \right) x_2 + h_{1m,0} n_{0,2}^{m*} - h_{2m,0}^{*} n_{0,1}^{m} - h_{1m,1}^{*} n_{1,1}^{m} + h_{2m,1} n_{1,2}^{m*}. \tag{3.14}$$

In other words, the proposed space-time spreading scheme with two transmit and M receive antennas achieves the same diversity order as the MRC with $4M$ diversity branches. An important feature of the proposed transmit diversity is that it will reduce to original transmit diversity schemes [4], [5], if the channel coefficients are fixed for the duration of two consecutive symbols. This is similar to the results in [36], except that here we only use two spreading codes per user. One can see that from (3.13) and (3.14) with $|h_{1m,0}|^2 = |h_{1m,1}|^2$ and $|h_{2m,0}|^2 = |h_{2m,1}|^2$, and hence no loss in performance is incurred if the channel is modelled as a slowly-fading one.

In the case of orthogonal codes, and considering the case of two transmit and one receive antennas, where from (3.13) and (3.14), we can write the probability of

bit error for the single-user conditioned on the channel coefficients according to

$$\begin{aligned} P_b(\hat{x}_1 = 1 \mid h_{11}^t, h_{21}^t, h_{11}^{t+T}, h_{21}^{t+T}) \\ &= Q\left(\sqrt{\frac{(|h_{11}^t|^2 + |h_{21}^t|^2 + |h_{11}^{t+T}|^2 + |h_{21}^{t+T}|^2)}{\sigma_n^2}}\right) \\ &= Q\left(\sqrt{\frac{2(|h_{11}^t|^2 + |h_{21}^t|^2 + |h_{11}^{t+T}|^2 + |h_{21}^{t+T}|^2)}{N_o}}\right) \end{aligned} \tag{3.15}$$

where σ_n^2 represents the variance of the independent complex AWGN samples, and the bit energy is assumed to be unity. The expression inside the square root in (3.15) is Chi-squared distributed according to (14.4-13) in [8] with eight degrees of freedom. Based on this, we define the signal to noise ratio per bit, γ_b as

$$\gamma_b = \frac{(|h_{11}^t|^2 + |h_{21}^t|^2 + |h_{11}^{t+T}|^2 + |h_{21}^{t+T}|^2)}{N_o}$$

with pdf given by

$$p(\gamma_b) = \frac{1}{6\bar{\gamma}_c^4}\gamma_b^3 e^{-\frac{\gamma_b}{\bar{\gamma}_c}} \tag{3.16}$$

where $\bar{\gamma}_c$ is the average signal to noise ratio per channel. That is

$$\bar{\gamma}_c = \frac{E(|h_k|^2)}{N_o}$$

and E denotes expectation operation. Averaging (3.15) over the pdf in (3.16), we

have [8]

$$P_b = \int_0^\infty Q(\sqrt{2\gamma_b}) p(\gamma_b) d\gamma_b$$

which yields to

$$P_b = \left[\frac{1}{2}(1-\mu)\right]^4 \sum_{k=0}^{3} \binom{3+k}{k} \left[\frac{1}{2}(1+\mu)\right]^k \tag{3.17}$$

where by definition

$$\mu = \sqrt{\frac{\bar{\gamma}_c}{1+\bar{\gamma}_c}}.$$

At high SNR, the term $\frac{1}{2}(1+\mu) \approx 1$ and the term $\frac{1}{2}(1-\mu) \approx \frac{1}{4\bar{\gamma}_c}$. Therefore, when $\bar{\gamma}_c$ is sufficiently large, the probability of error in (3.17) can be approximated by

$$P_b \approx \left(\frac{1}{4\bar{\gamma}_c}\right)^4 \binom{7}{4}. \tag{3.18}$$

The expression in (3.18) shows that the probability of error decreases in proportion with the factor $\frac{1}{\bar{\gamma}_c}$ raised to the power 4, hence the diversity order achieved is twofold of the one delivered using existing schemes [5].

3.4 Adaptive Space-Time Decoding

In the previous section, the proposed space-time spreading scheme was analyzed for the case when spreading codes are orthogonal. For a CDMA system, this requirement may be to optimistic, especially if the number of users is large. In what follows,

we examine the case when nonorthogonal codes are used. Note that the reason behind this study is to examine the effect of nonorthogonality of the spreading codes at the decoder side, and not at the transmitter. For this case, we propose a simple adaptive space-time decoder based on the MMSE criterion. The proposed adaptive MMSE receiver takes into account the signal interference due to the nonorthogonality of the code sequences. We also consider a fast-fading scenario where channel coefficients are independent from one-bit-to-another.

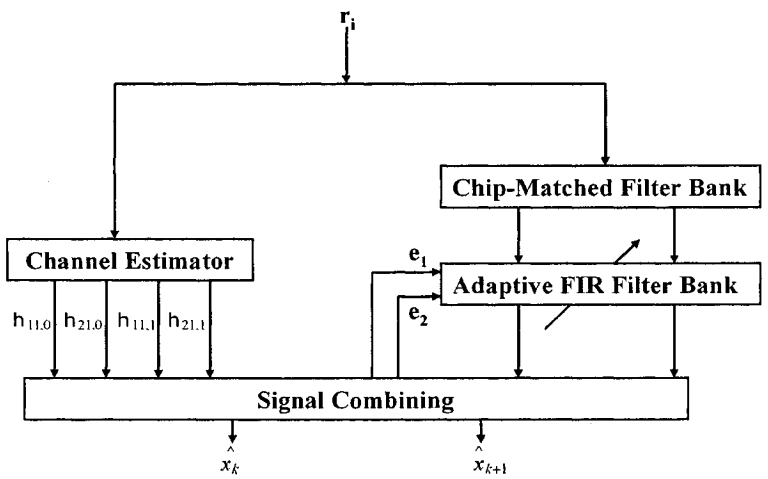

Figure 3.2: Adaptive combining for the nonorthogonal space-time spreading scheme.

The adaptive receiver is shown in Figure 3.2 where we use the normalized least-mean squares (NLMS) algorithm for filter tap weights adaptation. As shown, each chip-matched filter is followed by an adaptive MMSE finite-impulse response (FIR) filter. The output of these adaptive filters is coherently combined, and then a data decision is made. To alleviate the channel tracking problem of the standard adaptive MMSE receiver in fast-fading channels, we incorporate the channel coefficients into

the error signal fed-back to each filter as in [38].

3.5 Multiuser System Model

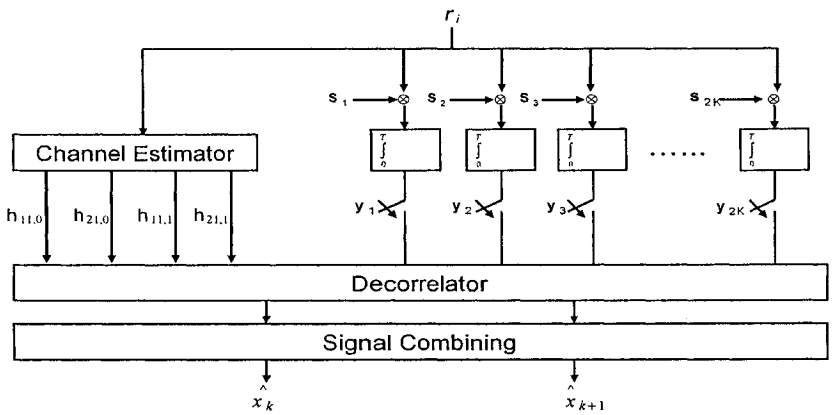

Figure 3.3: Multiuser receiver structure.

Considering a synchronous DS-CDMA system [39], and using vector notation, the single-user model discussed in Section 3.3 can be generalized to a K-user system. In what follows, we consider BPSK transmission and a fast-fading channel. In this case, the output of the $2K$ matched filters (shown in Figure 3.3) at the mth receive antenna can be expressed as

$$\mathbf{Y}_0^m = \mathbf{R}\mathbf{H}_0^m\mathbf{x} + \mathbf{N}_0^m \tag{3.19}$$

at time t, and as

$$\mathbf{Y}_1^m = \mathbf{R}\mathbf{H}_1^m\mathbf{x} + \mathbf{N}_1^m \tag{3.20}$$

at time $t+T$, respectively. In (3.19) and (3.20), the $(2K \times 1)$ vector $\mathbf{Y}_j^m$, $j = 0, 1$, represents the output of the bank of matched filters at times t and $t+T$, defined as

$$\mathbf{Y}_j^m = \left[y_{j,11}^m, y_{j,12}^m, ..., y_{j,k1}^m, y_{j,k2}^m, ..., y_{j,K1}^m, y_{j,K2}^m\right]^{\mathrm{T}} \tag{3.21}$$

where $y_{j,ki}^m$, $j = 0, 1$, $i = 1, 2$, represents the ith matched filter output of user k at times t and $t+T$. The cross-correlation matrix $\mathbf{R}$ is given by

$$\mathbf{R} = \begin{bmatrix} \rho_{1,1} & .... & \rho_{1,k} & .... & \rho_{1,2K} \\ \rho_{2,1} & .... & \rho_{2,k} & .... & \rho_{2,2K} \\ .... & .... & .... & .... & .... \\ .... & .... & .... & .... & .... \\ \rho_{2K,1} & .... & \rho_{2K,k} & .... & \rho_{2K,2K} \end{bmatrix}. \tag{3.22}$$

If we define

$$\mathbf{h}_{0,k}^m = \begin{bmatrix} h_{1m,0,k} & -h_{2m,0,k} \\ h_{2m,0,k} & h_{1m,0,k} \end{bmatrix}, \tag{3.23}$$

$$\mathbf{h}_{1,k}^m = \begin{bmatrix} h_{2m,1,k} & -h_{1m,1,k} \\ h_{1m,1,k} & h_{2m,1,k} \end{bmatrix}, \tag{3.24}$$

then, the $(2K \times 2K)$ channel coefficients matrix $\mathbf{H}_j^m$, $j = 0, 1$ in (3.19) is defined as

$$\mathbf{H}_j^m = \begin{bmatrix} \mathbf{h}_{j,1}^m & 0 & .... & 0 & 0 \\ 0 & \mathbf{h}_{j,2}^m & .... & 0 & 0 \\ .... & .... & .... & .... & .... \\ .... & .... & .... & ..\mathbf{h}_{j,K-1}^m.. & .... \\ 0 & 0 & .... & 0 & \mathbf{h}_{j,K}^m \end{bmatrix}. \tag{3.25}$$

The $(2K \times 1)$ transmitted data vector, $\mathbf{x}$, in (3.19), for the K-user system is given by

$$\mathbf{x} = [x_{1,1}, x_{1,2}, ..., x_{k,1}, x_{k,2}, ..., x_{K,1}, x_{K,2}]^{\mathrm{T}} \tag{3.26}$$

where $x_{k,i}$, $i = 1, 2$ represents the even and odd data symbols for user k. In (3.19) and (3.20), the $(2K \times 1)$ noise vector is defined as

$$\mathbf{N}_j^m = [N_{1,1}^m, N_{1,2}^m, ..., N_{k,1}^m, N_{k,2}^m, ..., N_{K,1}^m, N_{K,2}^m]^{\mathrm{T}} \tag{3.27}$$

where $\mathbf{N}_j^m$, $j = 0, 1$, consists of complex Gaussian random variables, $N_{k,i}^m$, $k = 1, ..., K$, $i = 1, 2$, each with variance $N_o/2$ per dimension. Given the matched filter outputs, the signals at times t and $t + T$ (i.e., $j = 0, 1$) are combined according to (3.11), (3.12). In general, for a K-user system, we can extract the two transmitted

symbols of user k, $\hat{x}_{k,1}$ and $\hat{x}_{k,2}$, from (3.19) and (3.20) as follows

$$\widehat{x}_{k,1} = \sum_{m=1}^{M} h_{1m,0,k} y_{0,k1}^{m*} + h_{2m,0,k}^{*} y_{0,k2}^{m} + h_{1m,1,k}^{*} y_{1,k2}^{m} + h_{2m,1,k} y_{1,k1}^{m*} \tag{3.28}$$

and

$$\widehat{x}_{k,2} = \sum_{m=1}^{M} h_{1m,0,k} y_{0,k2}^{m*} - h_{2m,0,k}^{*} y_{0,k1}^{m} - h_{1m,1,k}^{*} y_{1,k1}^{m} + h_{2m,1,k} y_{1,k2}^{m*}. \tag{3.29}$$

Note that, these data estimates are based on conventional matched filter detection which is only optimum if all users' codes are orthogonal (and among themselves). This orthogonality, of course, cannot be guaranteed especially if there exists a large number of users in the system. Even if this is possible, the orthogonality condition will be destroyed due to asynchronous transmission. To overcome this problem, we assume random spreading codes and use linear multiuser detection to compensate for the interference arising from signals cross-correlations. In this, we employ the decorrelator and the linear MMSE multiuser detectors before signal combining.

3.6 The Linear MMSE Detector

Here, we consider the MMSE multiuser detector. We determine the mapping Ω that minimizes the mean-square error (MSE) between transmitted and estimated

symbols according to

$$E[|\mathbf{x} - \hat{\mathbf{x}}|^2]. \tag{3.30}$$

Hence, the MMSE cost function can be expressed as

$$\begin{aligned}
\mathbf{J} &= E[|\mathbf{Hx} - \mathbf{\Omega Y}|^2] \\
&= E[(\mathbf{Hx} - \mathbf{\Omega Y})^H(\mathbf{Hx} - \mathbf{\Omega Y})] \\
&= E[\mathbf{x}^T\mathbf{H}^H\mathbf{Hx} - \mathbf{x}^T\mathbf{H}^H\mathbf{\Omega Y} - \mathbf{Y}^H\mathbf{\Omega}^H\mathbf{Hx} + \mathbf{Y}^H\mathbf{\Omega}^H\mathbf{\Omega Y}] \\
&= \mathbf{H}^H\mathbf{H}E[\mathbf{xx}^T] - 2E[\mathbf{x}^T\mathbf{H}^H\mathbf{\Omega Y}] + E[\mathbf{Y}^H\mathbf{\Omega}^H\mathbf{\Omega Y}] \\
&= trace\{E[\mathbf{xx}^T]\}\mathbf{H}^H\mathbf{H} - 2trace\{E[\mathbf{\Omega Y x}^T\mathbf{H}^H]\} + trace\{E[\mathbf{\Omega YY}^H\mathbf{\Omega}^H]\} \\
&= C - 2trace\{\mathbf{\Omega}E[\mathbf{Yx}^T\mathbf{H}^H]\} + trace\{\mathbf{\Omega}E[\mathbf{YY}^H]\mathbf{\Omega}^H\}
\end{aligned} \tag{3.31}$$

where trace(A) is the sum of the diagonal elements of matrix A,

$$\begin{aligned}
E[\mathbf{YY}^H] &= E[(\mathbf{RHx} + \mathbf{N})(\mathbf{RHx} + \mathbf{N})^H] = \mathbf{RH}E[\mathbf{xx}^T]\mathbf{H}^H\mathbf{R}^H + \sigma_n^2\mathbf{R} \\
&= \mathbf{RHH}^H\mathbf{R} + \sigma_n^2\mathbf{R}
\end{aligned} \tag{3.32}$$

and

$$E[\mathbf{Yx}^T\mathbf{H}^H] = E[(\mathbf{RHx} + \mathbf{N})\mathbf{x}^T\mathbf{H}^H] = \mathbf{RHH}^H. \tag{3.33}$$

Therefore, using (3.32) and (3.33), the MMSE cost function is given by

$$\begin{aligned}\mathbf{J} &= C - 2trace\{\mathbf{\Omega RHH}^H\} + trace\{\mathbf{\Omega}(\mathbf{RHH}^H\mathbf{R} + \sigma_n^2\mathbf{R})\mathbf{\Omega}^H\} \\ &= C - 2trace\{\mathbf{\Omega RHH}^H\} + trace\{\mathbf{\Omega RHH}^H\mathbf{R\Omega}^H\} + trace\{\sigma_n^2\mathbf{\Omega R\Omega}^H\} \quad (3.34)\end{aligned}$$

and by differentiating (3.34) with respect to $\mathbf{\Omega}$, we have

$$\mathbf{\Omega RHH}^H\mathbf{R} + \sigma_n^2\mathbf{\Omega R} = \mathbf{HH}^H\mathbf{R}.$$

Hence, it is straightforward to show that the linear MMSE-MUD is given by

$$\mathbf{\Omega} = (\mathbf{R} + \sigma_n^2(\mathbf{HH}^H)^{-1})^{-1}.$$

Although we discussed here the linear MMSE detector, but due to its complexity, in what follows we consider the performance analysis of the decorrelator MUD. As a matter of fact we can think about the decorrelator MUD performance as an upper bound for the MMSE detector.

3.7 Performance Analysis

For a K-user system, we can find the estimates of the transmitted symbols for user k at times t and $t+T$ by employing the decorrelator detector before signal combining.

Applying the decorrelator to the matched filter outputs in (3.19) and (3.20), we have

$$\underbrace{\mathbf{R}^{-1}\mathbf{Y}_0^m}_{\mathbf{Z}_0^m} = \mathbf{H}_0^m\mathbf{x} + \mathbf{R}^{-1}\mathbf{N}_0^m \tag{3.35}$$

$$\underbrace{\mathbf{R}^{-1}\mathbf{Y}_1^m}_{\mathbf{Z}_1^m} = \mathbf{H}_1^m\mathbf{x} + \mathbf{R}^{-1}\mathbf{N}_1^m \tag{3.36}$$

where $\mathbf{R}^{-1}$ is the inverse of the cross-correlation matrix defined in (3.22). The $(2K \times 1)$ vectors, $\mathbf{Z}_0^m = \mathbf{R}^{-1}\mathbf{Y}_0^m$ and $\mathbf{Z}_1^m = \mathbf{R}^{-1}\mathbf{Y}_1^m$ represent the output of the mth decorrelator at times $j = 0, 1$ respectively.

Without loss of generality, in what follows, we consider user 1 as the desired user and for brevity we drop its corresponding subscript. From (3.35) and (3.36) one can write the first and second elements of the vectors $\mathbf{Z}_0^m$ and $\mathbf{Z}_1^m$ as

$$Z_{11,0}^m = h_{11,0}^m x_1 - h_{21,0}^m x_2 + (\mathbf{R}^{-1}\mathbf{N}_0^m)_{11}$$

$$Z_{21,0}^m = h_{21,0}^m x_1 + h_{11,0}^m x_2 + (\mathbf{R}^{-1}\mathbf{N}_0^m)_{21},$$

$$Z_{11,1}^m = h_{21,1}^m x_1 - h_{11,1}^m x_2 + (\mathbf{R}^{-1}\mathbf{N}_1^m)_{11}$$

$$Z_{21,1}^m = h_{11,1}^m x_1 + h_{21,1}^m x_2 + (\mathbf{R}^{-1}\mathbf{N}_1^m)_{21}$$

where $Z_{i1,j}^m$, $(\mathbf{R}^{-1}\mathbf{N}_j^m)_{i1}$ with $i = 1, 2$, $j = 0, 1$ represent the ith element of the $(2K \times 1)$ vectors $\mathbf{Z}_j^m$, $\mathbf{R}^{-1}\mathbf{N}_j^m$, respectively. Now using the combining scheme in

(3.28) to find $\hat{x}_1$ (i.e., symbol 1 for user 1), we have

$$\begin{aligned}\hat{x}_1 = &(|h_{11,0}|^2 + |h_{21,0}|^2 + ... + |h_{1M,1}|^2 + |h_{2M,1}|^2)x_1 \\ &+ h_{11,0}(\mathbf{R}^{-1}\mathbf{N}_0^1)^*_{11} + h^*_{21,0}(\mathbf{R}^{-1}\mathbf{N}_0^1)_{21} + ... \\ &+ h_{1M,0}(\mathbf{R}^{-1}\mathbf{N}_0^M)^*_{1m} + h^*_{2M,0}(\mathbf{R}^{-1}\mathbf{N}_0^M)_{2M} \\ &+ h_{21,1}(\mathbf{R}^{-1}\mathbf{N}_1^1)^*_{11} + h^*_{11,1}(\mathbf{R}^{-1}\mathbf{N}_1^1)_{21} + ... \\ &+ h_{2M,1}(\mathbf{R}^{-1}\mathbf{N}_1^M)^*_{1M} + h^*_{1M,1}(\mathbf{R}^{-1}\mathbf{N}_1^M)_{2M}. \end{aligned} \tag{3.37}$$

We can generally express the probability of making an error conditioned on all channel coefficients from (3.37) as,

$$\begin{aligned}&P_b(\hat{x}_1 = 1 \mid h_{11,0}, h_{21,0}, ...h_{1M,1}, h_{2M,1}) \\ &\quad = Q\left(\frac{\sum_{m=1}^{M} |h_{1m,0}|^2 + |h_{2m,0}|^2 + |h_{1m,1}|^2 + |h_{2m,1}|^2}{\sqrt{\sigma^2_{\hat{x}_1}}}\right)\end{aligned} \tag{3.38}$$

where the Q-function is defined by

$$Q(x) = \int_x^\infty \frac{1}{\sqrt{2\pi}} \exp(-\frac{v^2}{2}) dv$$

and

$$\sigma^2_{\hat{x}_1} = \sigma^2_n \left[R^{-1}_{11} \left(\sum_{m=1}^{M} |h_{1m,0}|^2 + |h_{2m,1}|^2 \right) + R^{-1}_{22} \left(\sum_{m=1}^{M} |h_{2m,0}|^2 + |h_{1m,1}|^2 \right) \right]. \tag{3.39}$$

The parameters R_{11}^{-1} and R_{22}^{-1} in (3.39) denote the first and second elements of the diagonal of the inverse of the cross-correlation matrix respectively, and σ_n^2 is the variance of independent complex Gaussian noise samples. Substitution of (3.39) in (3.38) yields

$$P_b(\hat{x}_1 = 1 \mid h_{11,0}, h_{21,0}, ...h_{1M,1}, h_{2M,1})$$

$$= Q\left(\frac{\sum_{m=1}^{M} |h_{1m,0}|^2 + |h_{2m,0}|^2 + |h_{1m,1}|^2 + |h_{2m,1}|^2}{\sigma_n\sqrt{\left[R_{11}^{-1}\left(\sum_{m=1}^{M} |h_{1m,0}|^2 + |h_{2m,1}|^2\right) + R_{22}^{-1}\left(\sum_{m=1}^{M} |h_{2m,0}|^2 + |h_{1m,1}|^2\right)\right]}}\right). \tag{3.40}$$

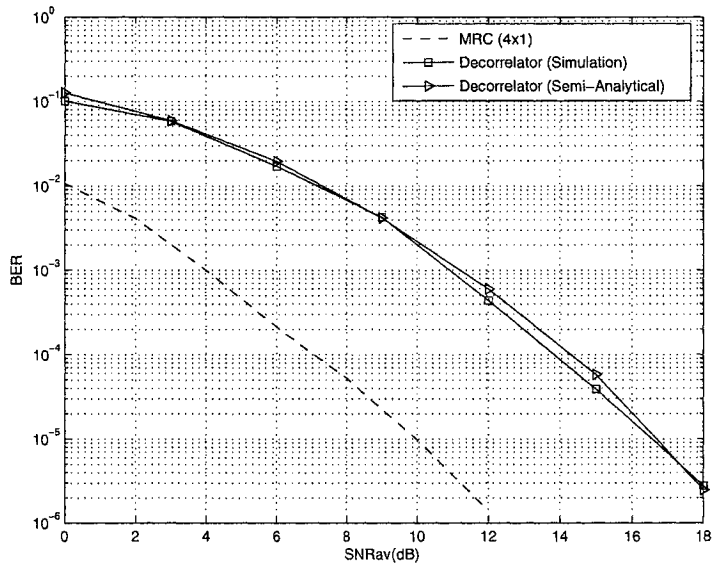

Figure 3.4: Simulation and semi-analytical results for user 1 in a 5-users DS-CDMA system.

Figure 3.4 depicts the simulation and semi-analytical results for user 1 in a 5-users DS-CDMA system that employs the proposed space-time transmission scheme. In the simulations, a BPSK modulation and 31-chips Gold codes are employed. The semi-analytical results are obtained using (3.40), where we generated and averaged over 10^6 random realizations of the channel coefficients for each simulation point. The generalization of the probability of error in (3.40) to the kth user is simply given by

$$P_b(\hat{x}_1 = 1 \mid h_{11,0}, h_{21,0}, ...h_{1M,1}, h_{2M,1}) = Q\left(\frac{\sum_{m=1}^{M} |h_{1m,0}|^2 + |h_{2m,0}|^2 + |h_{1m,1}|^2 + |h_{2m,1}|^2}{\sigma_n \sqrt{\left[R_{\psi}^{-1}\left(\sum_{m=1}^{M} |h_{1m,0}|^2 + |h_{2m,1}|^2\right) + R_{\theta}^{-1}\left(\sum_{m=1}^{M} |h_{2m,0}|^2 + |h_{1m,1}|^2\right)\right]}}\right) \tag{3.41}$$

where $\psi = (2k-1),(2k-1)$ and $\theta = 2k,2k$. It is worth to mention that we can check the validity of (3.41) by considering the single-user orthogonal case ($K = 1$). Obviously, when the signature sequences are orthogonal, the parameters $R^{-1}_{(2k-1),(2k-1)}$ and $R^{-1}_{2k,2k}$ are equal to one, then (3.41) will reduce to the single-user orthogonal expression.

To evaluate the probability of error in (3.41), one needs first to find the probability density function (pdf) of the corresponding SNR in (3.41). In what follows, we obtain this pdf.

3.7.1 Mathematical Model

Let us define two random variables (RVs) α_1 and α_2 as

$$\alpha_1 = \sum_{m=1}^{M} |h_{1m,0}|^2 + |h_{2m,1}|^2$$

$$\alpha_2 = \sum_{m=1}^{M} |h_{2m,0}|^2 + |h_{1m,1}|^2 .$$

In this case, α_1 and α_2 are chi-square distributed each with $4M$ degrees of freedom and pdf

$$f(\alpha_i) = \frac{1}{(2\sigma^2)^{2M}\,(2M-1)!}\alpha_i^{(2M-1)} \exp - \left(\frac{\alpha_i}{2\sigma^2}\right) \qquad \alpha_i \geq 0 \tag{3.42}$$

where σ^2 is the variance of the channel coefficients assumed to be 0.5 per dimension. By designating the two parameters R_ψ^{-1} and R_θ^{-1} as C_1, C_2 respectively, then the argument inside the Q-function in (3.41), renamed in terms of another RV β_1, can be written as

$$\beta_1 = \frac{\alpha_1 + \alpha_2}{\sqrt{C_1\alpha_1 + C_2\alpha_2}}. \tag{3.43}$$

Also, let us define a RV β_2 as

$$\beta_2 = C_1\alpha_1 + C_2\alpha_2. \tag{3.44}$$

Based on this model, next we show how to obtain the pdf of β_1.

3.7.2 Joint Density Function of β_1 and β_2

One way to obtain the pdf of β_1 is through the transformation of random variables. The first step is to determine the joint pdf of the random variables β_1 and β_2, $f(\beta_1, \beta_2)$ according to [41]

$$\begin{aligned} f(\beta_1, \beta_2) &= f(\alpha_1, \alpha_2)\,|\mathcal{L}(\beta_1, \beta_2)| \\ &= f(\alpha_1) f(\alpha_2)\,|\mathcal{L}(\beta_1, \beta_2)| \end{aligned} \tag{3.45}$$

where $|\mathcal{L}(\beta_1, \beta_2)|$ represents the absolute value of the Jacobian of the inverse transformation. Also it is clear that (3.45) is due to the independence of the RVs α_1 and α_2. Using (3.43) and (3.44), α_1 and α_2 can be expressed in terms of β_1 and β_2 as follows

$$\alpha_1 = \frac{C_2\beta_1\sqrt{\beta_2} - \beta_2}{|C_2 - C_1|} \tag{3.46}$$

$$\alpha_2 = \frac{C_1\beta_1\sqrt{\beta_2} - \beta_2}{|C_1 - C_2|}. \tag{3.47}$$

The Jacobian of the transformation in (3.45) is then given by

$$|\mathcal{L}(\beta_1, \beta_2)| = \frac{\sqrt{\beta_2}}{|C_1 - C_2|}. \tag{3.48}$$

Finally, after some algebraic manipulation, we have

$$f(\beta_1,\beta_2) = \lambda \sum_{k=0}^{2M-1}\sum_{j=0}^{2M-1}(-1)^{k+j}\binom{2M-1}{k}\binom{2M-1}{j} \tag{3.49}$$
$$C_2^{2M-k-1}C_1^{2M-j-1}\beta_1^{2(2M-1)-k-j}\beta_2^{2M+\frac{1}{2}(k+j-1)}\exp\left(-\frac{\beta_1\sqrt{\beta_2}}{2\sigma^2}\right)$$

where

$$\lambda = \frac{1}{(2\sigma^2)^{4M}\left[(2M-1)!\right]^2\left(|C_2-C_1|\right)^{4M-1}}.$$

It is straightforward to show that $min(C_1^2,C_2^2)\beta_1^2 \leq \beta_2 \leq max(C_1^2,C_2^2)\beta_1^2$, $0 \leq \beta_1 \leq \infty$.

3.7.3 Density Function of β_1

To perform the integration of (3.49) over β_2, we first introduce the following formula

$$\int_{c_1}^{c_2} x^n e^{-ax}dx = \frac{1}{a(n+1)}\left[c_2^n(ac_2)^{-\frac{n}{2}}e^{-\frac{ac_2}{2}}\mathbb{M}\left(\frac{n}{2},\frac{n+1}{2},ac_2\right)\right.$$
$$\left. -c_1^n(ac_1)^{-\frac{n}{2}}e^{-\frac{ac_1}{2}}\mathbb{M}\left(\frac{n}{2},\frac{n+1}{2},ac_1\right)\right] \tag{3.50}$$

where $\mathbb{M}(k,m,z)$ represents WhittakerM function defined as [42]

$$\mathbb{M}(k,m,z) = z^{\frac{1}{2}+m}e^{-\frac{z}{2}}\left[1+\frac{\frac{1}{2}+m-k}{1!(2m+1)}z+\frac{(\frac{1}{2}+m-k)(\frac{3}{2}+m-k)}{2!(2m+1)(2m+2)}z^2+.....\right].$$

Given this, the integration of (3.49) can be written as

$$I = \lambda \sum_{k=0}^{2M-1} \sum_{j=0}^{2M-1} (-1)^{k+j} \binom{2M-1}{k} \binom{2M-1}{j} C_2^{2M-k-1} C_1^{2M-j-1}$$
$$\beta_1^{2(2M-1)-k-j} \int_{C_1^2\beta_1^2}^{C_2^2\beta_1^2} \beta_2^{2M+\frac{1}{2}(k+j-1)} \exp\left(-\frac{\beta_1\sqrt{\beta_2}}{2\sigma^2}\right) d\beta_2. \tag{3.51}$$

Using the substitution $t = \sqrt{\beta_2}$, (3.51) can be expressed as

$$I = 2\lambda \sum_{k=0}^{2M-1} \sum_{j=0}^{2M-1} (-1)^{k+j} \binom{2M-1}{k} \binom{2M-1}{j} C_2^{2M-k-1} C_1^{2M-j-1}$$
$$\beta_1^{2(2M-1)-k-j} \int_{C_1\beta_1}^{C_2\beta_1} t^{4M+k+j} \exp\left(-\frac{\beta_1 t}{2\sigma^2}\right) dt \tag{3.52}$$

which can be easily solved using (3.50), to yield

$$I = 2\lambda \sum_{k=0}^{2M-1} \sum_{j=0}^{2M-1} \frac{(-1)^{k+j}}{4M+k+j+1} (2\sigma^2)^{2M+\frac{1}{2}(k+j+1)} \binom{2M-1}{k} \binom{2M-1}{j} C_2^{2M-k-1}$$
$$C_1^{2M-j-1} \beta_1^{4M-k-j-3} \left[C_2^{2M+\frac{1}{2}(k+j)} e^{-(\frac{C_2\beta_1^2}{4\sigma^2})} \mathbb{M}\left(2M+\frac{1}{2}(k+j), 2M+\frac{1}{2}(k+j)+\frac{1}{2}, \frac{C_2\beta_1^2}{2\sigma^2}\right) \right.$$
$$\left. - C_1^{2M+\frac{1}{2}(k+j)} e^{-(\frac{C_1\beta_1^2}{4\sigma^2})} \mathbb{M}\left(2M+\frac{1}{2}(k+j), 2M+\frac{1}{2}(k+j)+\frac{1}{2}, \frac{C_1\beta_1^2}{2\sigma^2}\right) \right]. \tag{3.53}$$

In terms of the well known confluent hypergeometric function [42, (13.1.32)], one can express (3.53) using

$$\mathbb{M}(k, m, z) = z^{\frac{1}{2}+m} e^{-\frac{z}{2}} \, {}_1F_1(m-k+\frac{1}{2}; 1+2m; z)$$

where

$$ {}_1F_1(a;b;z) = \sum_{n=0}^{\infty} \frac{(a)_n}{(b)_n} \frac{z^n}{n!} $$

is the confluent hypergeometric function with $(a)_n$ and $(b)_n$ being Pochhammer symbols. Hence, the pdf of β_1 is given by (shown in Figure 3.5)

$$ f(\beta_1) = 2\lambda \sum_{k=0}^{2M-1} \sum_{j=0}^{2M-1} \frac{(-1)^{k+j}}{4M+k+j+1} \binom{2M-1}{k} \binom{2M-1}{j} C_2^{2M-k-1} C_1^{2M-j-1} \beta_1^{8M-1} $$
$$ \left[C_2^{4M+k+j+1} e^{-(\frac{C_2\beta_1^2}{2\sigma^2})} \, {}_1F_1\left(1; 4M+k+j+2, \frac{C_2\beta_1^2}{2\sigma^2}\right) \right. $$
$$ \left. - C_1^{4M+k+j+1} e^{-(\frac{C_1\beta_1^2}{2\sigma^2})} \, {}_1F_1\left(1; 4M+k+j+2, \frac{C_1\beta_1^2}{2\sigma^2}\right) \right] \quad , \quad 0 \leq \beta_1 \leq \infty \qquad (3.54) $$

where for verification, we used numerical integration methods to check that the integration of the pdf in (3.54) tends to unity autonomous of the values of the parameters C_1 and C_2.

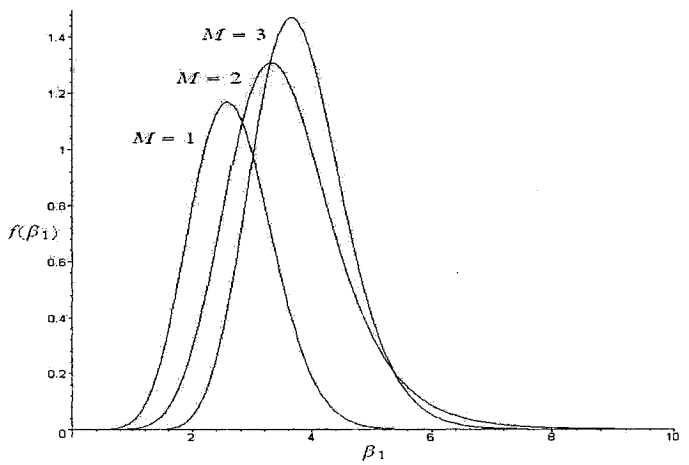

Figure 3.5: PDF of β_1 for 5 users, $N = 2$ and $M = 1, 2, 3$ antennas.

3.7.4 Probability of Error

Having obtained the pdf of β_1, one can find the probability of bit error by averaging (3.41) over the pdf found in (3.54) as

$$P_b = \int_0^\infty Q\left(\sqrt{\frac{2}{N_o}}\beta_1\right) f(\beta_1)\, d\beta_1. \tag{3.55}$$

Using the *preferred* form of the Q-function in [43]

$$Q(x) = \frac{1}{\pi}\int_0^{\frac{\pi}{2}} e^{-\frac{x^2}{2\sin^2\theta}} d\theta, \tag{3.56}$$

we have

$$\begin{aligned}
P_b &= \frac{1}{\pi}\int_0^{\frac{\pi}{2}}\int_0^\infty e^{-\frac{\beta_1^2}{N_o \sin^2\theta}} f(\beta_1) d\beta_1 d\theta \\
&= \frac{2\lambda}{\pi}\int_0^{\frac{\pi}{2}} \sum_{k=0}^{2M-1}\sum_{j=0}^{2M-1} \frac{(-1)^{k+j}}{4M+k+j+1}\binom{2M-1}{k}\binom{2M-1}{j} C_2^{2M-k-1} C_1^{2M-j-1} \\
&\int_0^\infty \beta_1^{8M-1} e^{-\frac{\beta_1^2}{N_o\sin^2\theta}} \left[C_2^{4M+k+j+1} e^{-(\frac{C_2\beta_1^2}{2\sigma^2})}\ {}_1F_1\left(1; 4M+k+j+2, \frac{C_2\beta_1^2}{2\sigma^2}\right)\right. \\
&\left. - C_1^{4M+k+j+1} e^{-(\frac{C_1\beta_1^2}{2\sigma^2})}\ {}_1F_1\left(1; 4M+k+j+2, \frac{C_1\beta_1^2}{2\sigma^2}\right)\right] d\beta_1 d\theta.
\end{aligned} \tag{3.57}$$

Finally, and as shown the Appendix A, the probability of error in (3.54) reduces to

$$
\begin{aligned}
P_b \;=\; & \frac{\lambda}{\pi}\sum_{k=0}^{2M-1}\sum_{j=0}^{2M-1}\frac{(-1)^{k+j}}{4M+k+j+1}\binom{2M-1}{k}\binom{2M-1}{j}C_2^{2M-k-1}C_1^{2M-j-1} \\
& \left(\frac{1}{\bar{\gamma}_c}\right)^{4M}\frac{\Gamma(4M+\frac{1}{2})\Gamma(\frac{1}{2})}{4M}\Big[C_2^{4M+k+j+1} \\
& {}_3F_2(4M+\frac{1}{2},4M+k+j+1,4M;4M+1,4M+k+j+2;-\frac{C_2}{\bar{\gamma}_c}) - C_1^{4M+k+j+1} \\
& {}_3F_2(4M+\frac{1}{2},4M+k+j+1,4M;4M+1,4M+k+j+2;-\frac{C_1}{\bar{\gamma}_c})\Big] \qquad (3.58)
\end{aligned}
$$

where the average SNR per channel $\bar{\gamma}_c = \frac{E(|h_k|^2)}{N_o}$, with E denote expectation, and ${}_3F_2(.,.;.;.)$ is a special case of the generalized hypergeometric function defined by [44, (9.14.1)]

$$
{}_pF_q(\alpha_1,\alpha_2,...,\alpha_p;\beta_1,\beta_2,...,\beta_q;z) = \sum_{k=0}^{\infty}\frac{(\alpha_1)_k(\alpha_2)_k...(\alpha_p)_k}{(\beta_1)_k(\beta_2)_k...(\beta_q)_k}\frac{z^k}{k!} \qquad (3.59)
$$

and $(\alpha_p)_k$, $(\beta_q)_k$ are Pochhammer symbols. The expression in (3.58) was implemented using Maple, which has the hypergeometric function as one of its built-in functions.

3.8 Simulation Results

In this section, we present performance results for the proposed space-time spreading scheme using both orthogonal and nonorthogonal spreading codes. For the purpose of this study, we only consider two antenna configurations: $N = 2$, $M = 1$ and

$N = 2$, $M = 2$ transmit and receive antennas respectively. In what follows, we list the remaining system parameters used in our simulations. Each user signal is encoded using two spreading codes taken from a family of Gold codes of length 31 chips, or else mentioned. BPSK modulation is used, with an assumption of perfect channel state information (CSI). Also, the channel is modelled as a fast-fading channel, where we assume that the channel coefficients to be independent from one-bit-to-another.

3.8.1 Single-User

First, we examine the performance of the proposed transmit diversity scheme for orthogonal codes using the conventional detector. The spreading codes used are of length 32 chips. Figure 3.6 shows the bit-error rate performance of the proposed transmit diversity scheme compared to MRC with two and four diversity branches. Also shown, as a benchmark, is the performance of the uncoded case (i.e., no diversity). As seen from these results, the proposed diversity scheme with $N = 2$ and $M = 1$ antennas achieves the same diversity order as the MRC with four diversity branches (1 Tx. and 4 Rx.). In other words, our space-time spreading scheme will always achieve a diversity order that is twofold of that of the MRC with N transmit and M receive antennas. Note that the 6 dB difference between the proposed transmit diversity scheme and the equivalent MRC with the same number of receiver diversity branches is simply due to the assumption of fixed transmission power as

in [36] (i.e., 3 dB relative to [4]).

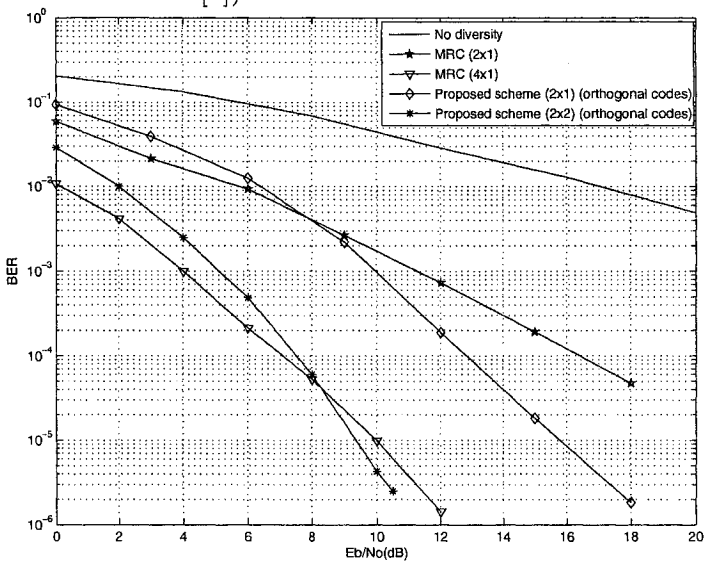

Figure 3.6: BER performance of the proposed transmit diversity for DS-CDMA systems in flat Rayleigh fading channels using orthogonal codes of length 32 chips.

Moving to the case of nonorthogonal spreading codes, we examine the performance of the proposed adaptive decoder discussed earlier. Also, as a reference, we include the performance of the ideal case of orthogonal codes. The results of this investigation are shown in Figures 3.7 and 3.8 for the BER and the frame error rate (FER), respectively. In Figure 3.8, we considered a frame length of 130 symbols. Two important remarks can be drawn from these results: (i) using the adaptive space-time block decoder, the diversity order of the underlying space-time code is still maintained even if the codewords are not orthogonal. (ii) the SNR loss incurred due to nonorthogonality is quite small, and can be easily compensated using error-control coding.

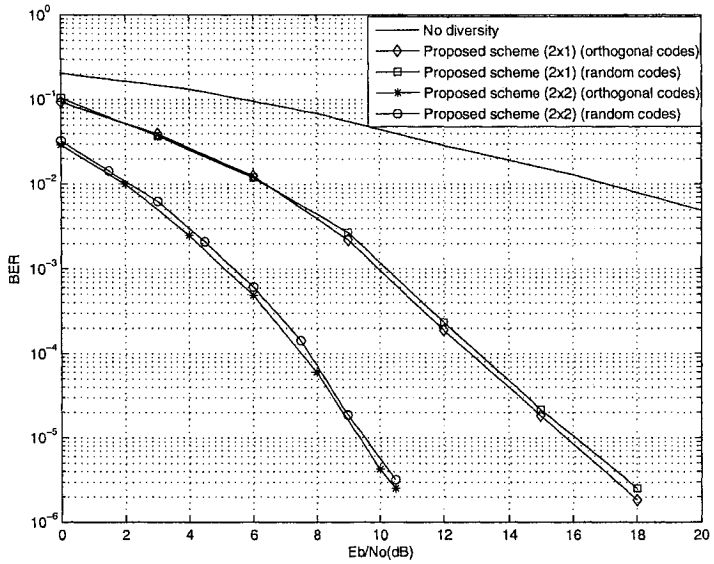

Figure 3.7: BER performance of the adaptive MMSE receiver in DS-CDMA system over flat fast-fading channels with random spreading codes of length 32 chips.

It is important to mention that both the receiver structures proposed in this chapter are based on perfect knowledge of the channel state information at the receiver side. Even though this assumption may be to optimistic especially if the channel is modelled as a fast fading-one, it can still be used as a benchmark for future studies where practical non-coherent combining techniques can be used [46], [47].

In Figure 3.9, we present the system performance using orthogonal codes of length 32 chips. Since here we only consider the single user case (no multiuser interference) with two orthogonal spreading codes, we refer to this as the single-user bound. As seen from the results in Figure 3.9, the proposed space-time spreading

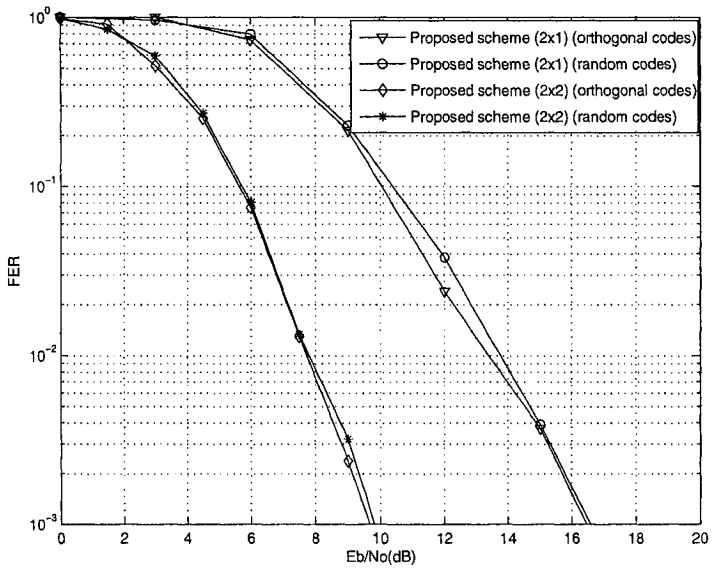

Figure 3.8: FER performance of the adaptive receiver in DS-CDMA system over flat fast-fading channels with random spreading codes of length 32 chips.

scheme with two transmit and one receive antenna delivers the same diversity order as the MRC with four diversity branches. As a benchmark, the MRC with two diversity branches, and no diversity cases are also shown in Figure 3.9. Also shown is the performance analysis for the single-user case given in (3.17), which confirms our previous conjunctures. In general, for N transmit and M receiving antennas, the space-time spreading scheme in Section 3.3 achieves twofold of the diversity order of that of the MRC.

3.8.2 Multiuser System

To examine the effect of multiple-access interference in a multiuser DS-CDMA system, we consider the case where all users spreading codes are random. In what follows, we present a simulation comparison between the decorrelator, MMSE and the

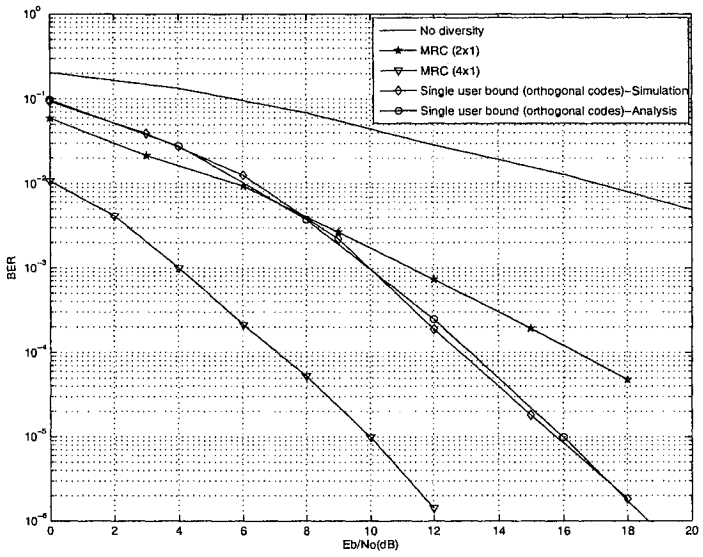

Figure 3.9: BER performance in flat Rayleigh fading channels, for orthogonal codes of length 32 chips

adaptive MMSE detectors. As shown in Figure 3.3, the output of the $2K$ matched filters is passed through an interference cancellation stage. Then, with appropriate combining of the output vector for each user, users' data can be extracted. As shown in Figure 3.10, both the decorrelator and the centralized MMSE receivers achieve the same diversity order as the MRC with four diversity branches. The adaptive NLMS based receiver [22], [38] offers the same diversity order with only a small SNR loss is incurred at low BERs. More interestingly, we show that using the adaptive combining scheme, the system only suffers from SNR degradation but no diversity loss is incurred. Since original STC are initially designed to provide diversity gain and not SNR gain, one can concatenate the proposed adaptive transmit diversity

scheme with a powerful error-control code to achieve large SNR gains (e.g., [28] and reference therein).

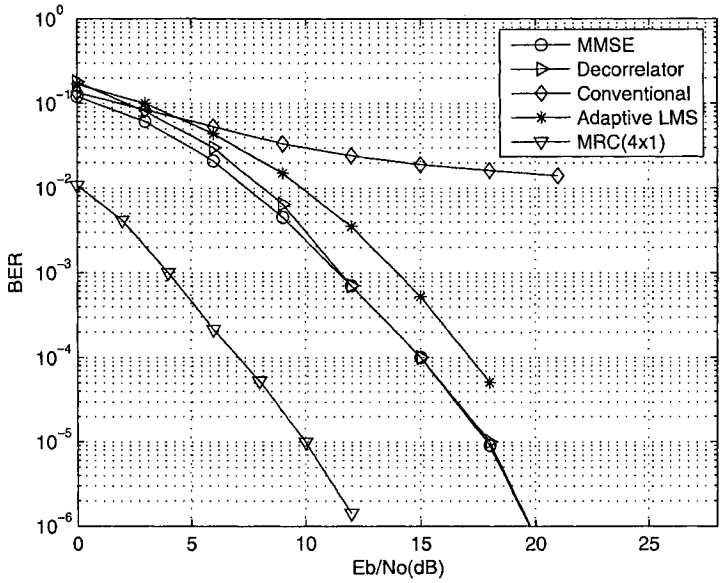

Figure 3.10: BER performance of the conventional, decorrelator, MMSE-MUD, and the adaptive MMSE receivers in a 5-user DS-CDMA system with random codes of length 32 chips.

Here we incorporate the adaptive NLMS receiver [38] with the proposed scheme for the multiuser case. In Figure 3.11, the effect of multiuser interference arising from the nonorthogonal codes is studied for different number of users. As seen from these results, using the proposed adaptive decoder, no diversity loss is incurred for systems with moderate number of users.

In Figure 3.12 , we examine the performance of the space-time system using both simulations and analytical results for a DS-CDMA system with different number of users and for the case of $N = 2$ and $M = 1$ antenna configuration. Also shown, as benchmarks, are the performance results for the single-user system and

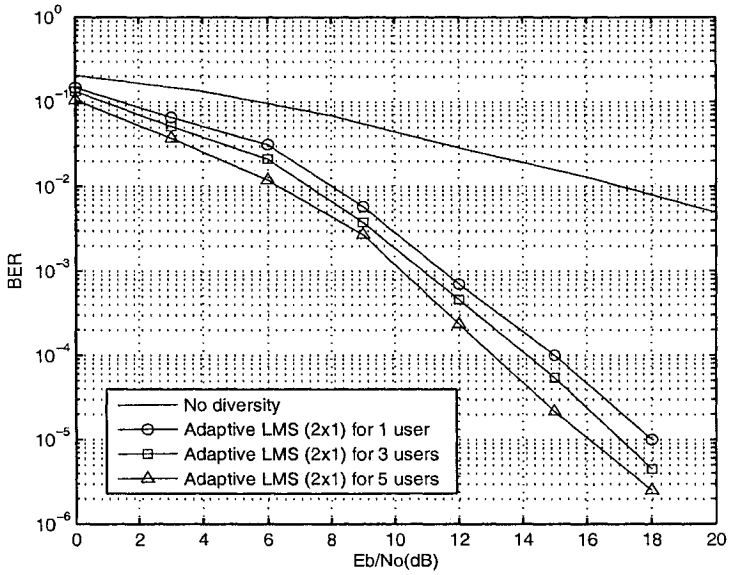

Figure 3.11: BER performance of the adaptive combining scheme for different system loads and using random spreading codes of length 32 chips.

the MRC with four diversity branches. Comparing the analytical results obtained using (3.58) to the simulations, one can see that the BER expression in (3.58) is quite accurate. Figure 3.13 presents the same results as in Figure 3.12 but with different antenna configuration ($N = 2$ and $M = 2$). Note that in both Figures 3.12 and 3.13, we refer to the single-user with orthogonal codes as the single-user bound. From these results, one can see that the full diversity order is always maintained regardless of the number of users (i.e., $2NM$=4 in Figure 3.12 and $2NM$=8 in Figure 3.13). Also note that the performance of the single-user system is 6 dB far from the MRC. This SNR loss is simply due to the fixed power constraint set at the transmitter side (i.e., two transmitted symbols per antenna for one transmission

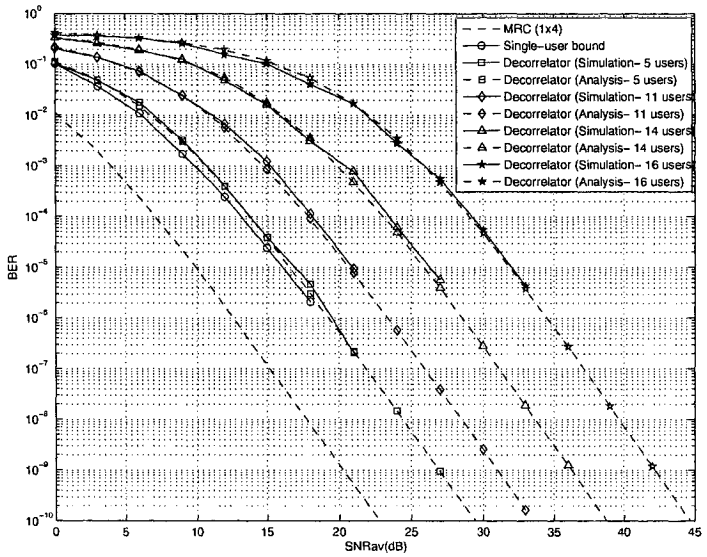

Figure 3.12: BER performance for N=2, M=1 antenna configuration over Rayleigh fast-fading channels.

period).

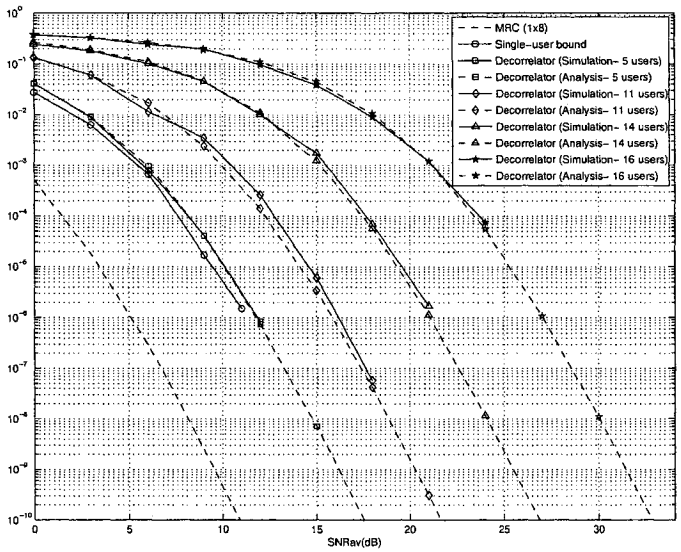

Figure 3.13: BER performance for N=2, M=2 antenna configuration over Rayleigh fast-fading channels.

In Figure 3.14, we examine the performance of the space-time system with $N = 2$, $M = 2$ antennas as a function of the number of users and for a fixed SNR of 12 dB.

3.9 Conclusion

In this Chapter, a simple transmit diversity scheme for CDMA systems based on space-time spreading, that exploits both spatial and temporal diversities for fast-fading channels, was introduced. We have proved that, with the same number of antennas as the MRC, the proposed coding scheme is able to achieve the full diversity promised by the channel (i.e., spatial and temporal). In that, we developed

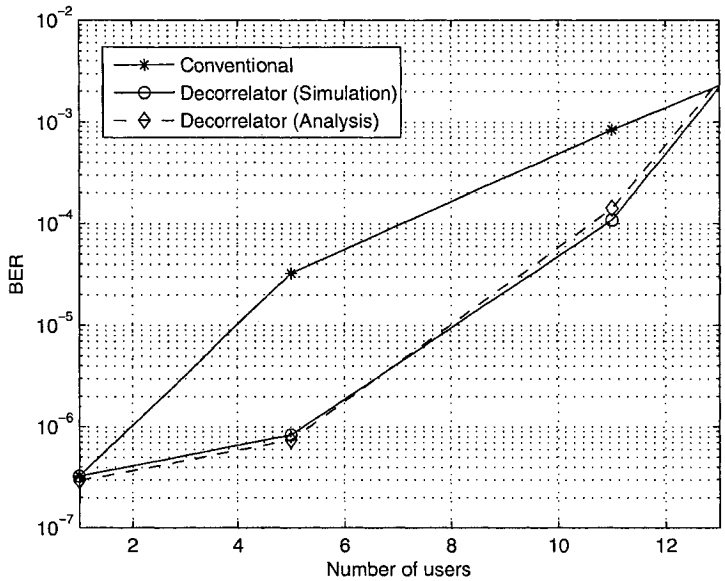

Figure 3.14: BER performance as a function of the number of users over fast-fading channels. N=2 and M=2 antennas and SNR=12 dB.

a semi-analytical model that provides a general representation of the performance analysis of the proposed space-time transmission scheme. By comparison with simulations the accuracy of this model was investigated in a DS-CDMA system using the decorrelator multiuser detector. Using our analytical results, and for the two channel models, we proved that the diversity order of the underlying scheme is always maintained regardless of the system load.

Chapter 4

Space-Time Spreading over Slow-Fading Channels

In Chapter 3, we proposed a space-time spreading scheme designed for fast-fading channels. In this chapter, we examine the the performance of the proposed scheme in slow-fading channels.

This chapter is organized as follows. In Section 4.1 we present previous works and list the contributions of this chapter. Section 4.2 introduces the system model for the single-user case using the proposed scheme over slow-fading channels. The multiuser system model is then given in Section 4.3. Section 4.4 provides the derivation of the probability of bit error for the proposed scheme using the decorrelator detector over slow-fading channels. Simulations and theoretical results are compared in Section 4.5. Finally, Section 4.6 concludes this chapter.

4.1 Introduction

4.1.1 Previous Work

Since the initial proposal of STCs, significant research efforts have aimed at the integration of these codes with DS-CDMA systems [48]-[50]. An application of STBC to wideband CDMA systems under the assumption of perfectly known channels was investigated in [49]. Also in [49], a maximum likelihood multiuser detection scheme for CDMA systems using orthogonal spreading codes was proposed. In [51], the performance of a STBC in a DS-CDMA system that uses the Rake receiver was investigated, while in [52] the same study is performed for different types of multiuser detectors. Furthermore, in [53] a successive interference cancellation multiuser detector was introduced to reduce the effect of MAI in a STBC system. A blind multiuser detector for asynchronous DS-CDMA systems with STBCs was also introduced in [54] for multipath channels. All these works have examined the optimization of STBC in DS-CDMA systems using joint space-time coding and multiuser detection.

4.1.2 Contribution

In the previous chapter we examined the performance of the proposed space-time transmit diversity scheme in fast-fading channels, while in this chapter this study is performed in a DS-CDMA system over slowly-fading channels. The underlying space-time system employs two transmit antennas and M receive antennas at the

user side and base-station receiver, respectively. To combat the effect of multiuser interference, we employ the linear decorrelator multiuser detector. In our analysis, we derive a closed form expression for the bit error probability. These theoretical results are shown to be very accurate when compared to system simulations. Both simulations and analytical results show that, regardless of the system load, the full diversity order of NM is always maintained and only a signal-to-noise ratio (SNR) loss is incurred when using a decorrelator detector at the receiver side. Using our theoretical results, we show that the loss in SNR from the single-user bound is upper bounded by $10\log(C/2)$ where (C) represents the sum of the two consecutive diagonal elements of the inverse of the cross-correlation matrix for the user under consideration.

4.2 System Model

We consider an uplink DS-CDMA scenario with two transmit and M receive antennas. At the transmitter side, we employ the space-time spreading scheme in Section 3.3 designed for fast-fading channels. However here, we examine the performance of this space-time spreading scheme over slowly-fading channels.

4.2.1 Space-Time Spreading and Encoder Design

The fast-fading channel system model introduced in Section 3.3, can be easily applied to slow-fading channels by assuming fixed channel coefficients for the duration of

two consecutive symbols. Hence, in what follows we drop the time dependence subscript (i.e., $h_{1m,0} = h_{1m,1} = h_{1m}$ and $h_{2m,0} = h_{2m,1} = h_{2m}$). Accordingly, the proposed space-time spreading scheme can be described as follows. If we let x_1 and x_2 be the input symbols to the encoder, then each data symbol is modulated using two spreading codes, s_i, $i = 1, 2$ followed by an addition operation to form the space-time code matrix

$$\begin{array}{lcc} & \text{Tx Antenna (1)} & \text{Tx Antenna (2)} \\ t = 0, & x_1^* s_1 + x_2^* s_2 & x_1 s_2 - x_2 s_1 \\ t = T, & x_1 s_2 - x_2 s_1 & x_1^* s_1 + x_2^* s_2. \end{array} \tag{4.1}$$

As seen from the code matrix in (4.1), the encoder produces codewords $x_1^* s_1 + x_2^* s_2$ and $x_1 s_2 - x_2 s_1$ to be transmitted from antenna 1 and 2, respectively, during the first transmission period. In the second transmission period, these codewords are switched with respect to the antenna order.

4.2.2 Space-Time Spreading and Decoder Design

At the receiver side, the received signal at the mth receive antenna can be written as

$$r_0^m = h_{1,m}(x_1^* s_1 + x_2^* s_2) + h_{2,m}(x_1 s_2 - x_2 s_1) + n_0^m \tag{4.2}$$

at time t, and as

$$r_1^m = h_{1,m}(x_1 s_2 - x_2 s_1) + h_{2,m}(x_1^* s_1 + x_2^* s_2) + n_1^m \tag{4.3}$$

at time $t+T$, where the noise n_0^m, n_1^m are modelled as independent samples of zero-mean complex Gaussian random variables, each with variance $\sigma_n^2 = N_0/2$ per dimension. In (4.2) and (4.3), the coefficients $h_{nm} = \alpha_{nm} e^{j\theta_{nm}}$ model the fading between the n^{th}, $n = 1, 2$, transmit and m^{th}, $m = 1, ..., M$ receive antenna, and are assumed to be independent complex Gaussian random variables with variance 0.5 per dimension.

Before signal combining, the received signals in (4.2) and (4.3) are first applied to a bank of two matched filters where each filter is matched to one of the two assigned code sequences. The output of these filters, after sampling, is given in a vector form by

$$\mathbf{y}_0^m = \mathbf{X}_0 \mathbf{h}^m + \mathbf{N}_0 \tag{4.4}$$

at time t, and by

$$\mathbf{y}_1^m = \mathbf{X}_1 \mathbf{h}^m + \mathbf{N}_1 \tag{4.5}$$

at time $t+T$, where $\mathbf{y}_0^m$ and $\mathbf{y}_1^m$ are (2×1) vectors with elements $y_{0,i}^m$, $y_{1,i}^m$, $i = 1, 2$.

In (4.4) and (4.5),

$$\mathbf{X}_0 = \begin{bmatrix} x_1^* + x_2^*\rho_{12} & x_1\rho_{12} - x_2 \\ x_1^*\rho_{21} + x_2^* & x_1 - x_2\rho_{21} \end{bmatrix},$$

$$\mathbf{X}_1 = \begin{bmatrix} x_1\rho_{12} - x_2 & x_1^* + x_2^*\rho_{12} \\ x_1 - x_2\rho_{21} & x_1^*\rho_{21} + x_2^* \end{bmatrix}, \tag{4.6}$$

where ρ_{ij} is the cross-correlation between the ith and jth spreading codes, the (2×1) vector $\mathbf{h}^m$ represents the channel coefficients with elements h_{nm}, $n = 1, 2$, $m = 1, ..., M$ while $N_{0,i}$ and $N_{1,i}$, $i = 1, 2$ are complex Gaussian random variables, each with variance $N_o/2$ per dimension. Now, assuming perfect channel estimation, the receiver performs signal combining on the output of the matched filter bank according to

$$\widehat{x}_1 = \sum_{m=1}^{M} h_{1m}y_{0,1}^{m*} + h_{2m}^*y_{0,2}^m + h_{1m}^*y_{1,2}^m + h_{2m}y_{1,1}^{m*} \tag{4.7}$$

$$\widehat{x}_2 = \sum_{m=1}^{M} h_{1m}y_{0,2}^{m*} - h_{2m}^*y_{0,1}^m - h_{1m}^*y_{1,1}^m + h_{2m}y_{1,2}^{m*}. \tag{4.8}$$

Assuming orthogonal spreading waveforms, the data estimates in (4.7) and (4.8) are

given by

$$\widehat{x}_1 = \sum_{m=1}^{M} 2\left(|h_{1m}|^2 + |h_{2m}|^2\right) x_1 + h_{1m} n_0^{m*} + h_{2m}^* n_0^m + h_{1m}^* n_1^m + h_{2m} n_1^{m*} \tag{4.9}$$

$$\widehat{x}_2 = \sum_{m=1}^{M} 2\left(|h_{1m}|^2 + |h_{2m}|^2\right) x_2 + h_{1m} n_0^{m*} - h_{2m}^* n_0^m - h_{1m}^* n_1^m + h_{2m} n_1^{m*}. \tag{4.10}$$

Note that, for the slowly-fading channel considered here, the space-time spreading scheme in Section 3.3 with two transmit and M receive antennas achieves the same diversity order as the MRC with $2M$ diversity branches. This confirms that the space-time spreading scheme in Section 3.3 offers no diversity loss, and hence reduces to existing space-time spreading scheme when the channel is modelled as slowly-fading.

At this point, it is important to mention that the result in our previous discussion we only considered the case of two transmit diversity at the user side merely for practical implications. However, generalization of the above results the case of N transmit diversity is straightforward.

4.3 Multiuser System Model

Considering a synchronous DS-CDMA system, and using vector notation, the single-user model can be generalized for the multiuser DS-CDMA system with K users. To simplify the notation, in what follows, we consider BPSK transmission. In this case, the output of the $2K$ matched filters at the mth receive antenna can be expressed as

$$\mathbf{Y}_0^m = \mathbf{R}\mathbf{H}_0^m\mathbf{x} + \mathbf{N}_0^m \tag{4.11}$$

at time t, and as

$$\mathbf{Y}_1^m = \mathbf{R}\mathbf{H}_1^m\mathbf{x} + \mathbf{N}_1^m \tag{4.12}$$

at time $t+T$, respectively. In (4.11) and (4.12), the $(2K \times 1)$ vectors $\mathbf{x}$, $\mathbf{Y}_i^m$, $i = 0, 1$, hold the same definitions as in (3.21) and (3.26) of Section 3.5. Also, the $(2K \times 2K)$ cross-correlation matrix $\mathbf{R}$ have the same definition of (3.22) mentioned in Section 3.5. If we define

$$\mathbf{h}_{0,k}^m = \begin{bmatrix} h_{1m,k} & -h_{2m,k} \\ h_{2m,k} & h_{1m,k} \end{bmatrix} \quad \text{and} \quad \mathbf{h}_{1,k}^m = \begin{bmatrix} h_{2m,k} & -h_{1m,k} \\ h_{1m,k} & h_{2m,k} \end{bmatrix} \tag{4.13}$$

then, the $(2K \times 2K)$ channel coefficients matrix $\mathbf{H}_i^m$, $i = 1, 2$ in (4.11) and (4.12), is defined as

$$\mathbf{H}_i^m = \begin{bmatrix} \mathbf{h}_{i,1}^m & 0 & .... & 0 & 0 \\ 0 & \mathbf{h}_{i,2}^m & .... & 0 & 0 \\ .... & .... & .... & .... & .... \\ .... & .... & .... & ..\mathbf{h}_{i,K-1}^m.. & .... \\ 0 & 0 & .... & 0 & \mathbf{h}_{i,K}^m \end{bmatrix}. \tag{4.14}$$

The $(2K \times 1)$ noise vector $\mathbf{N}_i^m$, $i = 1, 2$, consists of $N_{i,kj}^m$, $k = 1, ..., K$, $j = 1, 2$ complex Gaussian random variables, each with variance $N_o/2$ per dimension. Given the matched filter outputs, the signals at times t and $t + T$ (i.e., $i = 0, 1$) are combined according to (4.9), (4.10). In general, we can extract the two transmitted symbols of user k, $\hat{x}_{k,1}$ and $\hat{x}_{k,2}$, from (4.11) and (4.12) as follows

$$\widehat{x}_{k,1} = \sum_{m=1}^{M} h_{1m,k} y_{0,k1}^{m*} + h_{2m,k}^* y_{0,k2}^m + h_{1m,k}^* y_{1,k2}^m + h_{2m,k} y_{1,k1}^{m*} \tag{4.15}$$

and

$$\widehat{x}_{k,2} = \sum_{m=1}^{M} h_{1m,k} y_{0,k2}^{m*} - h_{2m,k}^* y_{0,k1}^m - h_{1m,k}^* y_{1,k1}^m + h_{2m,k} y_{1,k2}^{m*}. \tag{4.16}$$

4.4 Performance Analysis

In what follows, we derive the probability of error for a system that employs multi-user detection using the decorrelator detector.

For a K-user system that employs the decorrelator detector as a multiuser detector after the bank of matched filter, and before the signal combining scheme in (4.15) and (4.16), we have

$$\begin{aligned}
\underbrace{\mathbf{R}^{-1}\mathbf{Y}_0^1}_{\mathbf{Z}_0^1} &= \mathbf{H}_0^1\mathbf{x} + \mathbf{R}^{-1}\mathbf{N}_0^1 \\
&\vdots \\
\underbrace{\mathbf{R}^{-1}\mathbf{Y}_0^M}_{\mathbf{Z}_0^M} &= \mathbf{H}_0^M\mathbf{x} + \mathbf{R}^{-1}\mathbf{N}_0^M \qquad (4.17) \\
\underbrace{\mathbf{R}^{-1}\mathbf{Y}_1^1}_{\mathbf{Z}_1^1} &= \mathbf{H}_1^1\mathbf{x} + \mathbf{R}^{-1}\mathbf{N}_1^1 \\
&\vdots \\
\underbrace{\mathbf{R}^{-1}\mathbf{Y}_1^M}_{\mathbf{Z}_1^M} &= \mathbf{H}_1^M\mathbf{x} + \mathbf{R}^{-1}\mathbf{N}_1^M \qquad (4.18)
\end{aligned}$$

where the decorrelator mapping $\mathbf{M} = \mathbf{R}^{-1}$ represents the inverse of the cross-correlation matrix defined in (3.22). The $(2K \times 1)$ vectors, $\mathbf{Z}_0^m = \mathbf{R}^{-1}\mathbf{Y}_0^m$ and $\mathbf{Z}_1^m = \mathbf{R}^{-1}\mathbf{Y}_1^m$ represent the mth decorrelator output at times $i = 0, 1$ respectively.

Let us consider user 1 as the desired user and for brevity we drop its corresponding subscript. Using the appropriate combining scheme to find $\hat{x}_1$ (i.e., symbol

1 for user 1), yields

$$\begin{aligned}\hat{x}_1 = 2(|h_{11}|^2 + |h_{21}|^2 + ... + |h_{1M}|^2 + |h_{2M}|^2)x_1 \\ + h_{11}(\mathbf{R}^{-1}\mathbf{N}_0^1)^*_{11} + h^*_{21}(\mathbf{R}^{-1}\mathbf{N}_0^1)_{21} + ... \\ + h_{1M}(\mathbf{R}^{-1}\mathbf{N}_0^M)^*_{1M} + h^*_{2M}(\mathbf{R}^{-1}\mathbf{N}_0^M)_{2M} \\ + h_{21}(\mathbf{R}^{-1}\mathbf{N}_1^1)^*_{11} + h^*_{11}(\mathbf{R}^{-1}\mathbf{N}_1^1)_{21} + ... \\ + h_{2M}(\mathbf{R}^{-1}\mathbf{N}_1^M)^*_{1M} + h^*_{1M}(\mathbf{R}^{-1}\mathbf{N}_1^M)_{2M}. \end{aligned} \tag{4.19}$$

We can generally express the probability of making an error in $\hat{x}_1$ conditioned on the channel coefficients from (4.19) as

$$\begin{aligned}P_b(\hat{x}_1 = 1 \mid h_{11}, h_{21}, ..., h_{2M}) \\ = Q\left(\frac{2\sum_{m=1}^{M}|h_{1m}|^2 + |h_{2m}|^2}{\sqrt{\sigma^2_{\hat{x}_1}}}\right).\end{aligned} \tag{4.20}$$

From (4.19) it is easy to show that

$$\sigma^2_{\hat{x}_1} = \sigma^2_n\left(R^{-1}_{11} + R^{-1}_{22}\right)\sum_{m=1}^{M}|h_{1m}|^2 + |h_{2m}|^2 \tag{4.21}$$

where by R^{-1}_{11}, R^{-1}_{22} we indicate to the first and second elements of the diagonal of the inverse of the cross-correlation matrix respectively, and σ^2_n is the variance of independent complex AWGN samples. If we denote the sum of the two elements

R_{11}^{-1} and R_{22}^{-1} by C, then substituting (4.21) into (4.20) yields

$$P_b(\hat{x}_1 = 1 \mid h_{11}, h_{21}, ..., h_{2M}) = Q\left(2\sqrt{\frac{2\sum_{m=1}^{M}|h_{1m}|^2 + |h_{2m}|^2}{N_o C}}\right). \tag{4.22}$$

If we define γ_b as

$$\gamma_b = \frac{1}{N_o}\sum_{m=1}^{M}|h_{1m}|^2 + |h_{2m}|^2$$

with pdf given by [8]

$$p(\gamma_b) = \frac{1}{\bar{\gamma}_c^{2M}\,(2M-1)!}\gamma_b^{(2M-1)}e^{-\frac{\gamma_b}{\bar{\gamma}_c}}. \tag{4.23}$$

Then by averaging (4.22) over (4.23), we have

$$P_b = \int_0^\infty Q\left(2\sqrt{\frac{2\gamma_b}{C}}\right)p\left(\gamma_b\right)d\gamma_b$$

and finally [8]

$$P_b = \left[\frac{1}{2}\left(1-\mu\right)\right]^{2M}\sum_{k=0}^{2M-1}\binom{2M-1+k}{k}\left[\frac{1}{2}\left(1+\mu\right)\right]^k \tag{4.24}$$

where by definition

$$\mu = \sqrt{\frac{4\bar{\gamma}_c/C}{1+4\bar{\gamma}_c/C}}$$

and $\bar{\gamma}_c$ is the average signal-to-noise ratio per channel. That is

$$\bar{\gamma}_c = \frac{E(|h_{nm}|^2)}{N_o}$$

where E denotes the expectation operator.

Let us now examine the asymptotic behavior of the BER expression in (4.24). From (4.24) and at high SNRs where $\bar{\gamma}_c \ggg C$, the term $\frac{1}{2}(1+\mu) \approx 1$ and the term $\frac{1}{2}(1-\mu) \approx \frac{C}{4\bar{\gamma}_c}$. Therefore, when $\bar{\gamma}_c$ is sufficiently large, the probability of error in (4.24) can be approximated by

$$P_b \approx \left(\frac{C}{4\bar{\gamma}_c}\right)^{2M} \binom{4M-1}{2M}. \tag{4.25}$$

Three important remarks on the asymptotic BER expression (4.25) are: (i) The probability of error decreases in proportion to $\frac{1}{\bar{\gamma}_c}$ raised to the power $2M$, confirming that the proposed transmit diversity scheme achieves a diversity order of $2M$ when the channel is modelled as slowly-fading, (ii) Relative to the single-user bound, only a SNR loss bounded by $10\log(C/2)$ is incurred[1]. (iii) This SNR loss is *only* a function of the cross correlations among users, and independent of the number of transmit and/or receive antennas, N and M. These remarks will be explored further when we present our simulation results.

[1]Note that by the single-user bound, we mean the single-user system with two orthogonal spreading codes. In this case the parameter C=2.

4.5 Simulation Results

To examine the performance of the prescribed space-time system using both theoretical and simulation results, we use the following system parameters. Each user signal is encoded using two spreading codes taken from a family of Gold codes of length 31 chips. BPSK modulation is used, with an assumption of perfect channel state information. The channel is modelled as a slow-fading one, where the channel coefficient is fixed within a frame length of 130 symbols and change from one frame to another. For the simulation part, similar to Chapter 3, we only consider two antenna configurations; $N = 2$, $M = 1$ and $N = 2$, $M = 2$ transmit and receive antennas respectively.

4.5.1 Probability of Bit Error

In Figure 4.1, we compare the simulations with the analytical results in (4.24) for a DS-CDMA system with different number of users and for the case of $N = 2$ and $M = 1$ antenna configuration. Also shown, as benchmarks, are the performance results for the single-user system and the MRC with two diversity branches. Comparing the analytical results to the simulations, one can see that the BER expression in (4.24) is quite accurate.

Considering the $N = 2$ and $M = 2$ antenna configuration, Figure 4.2 shows the same results as in Figure 4.1. Note that in both Figures 4.1 and 4.2, we refer to the single-user with orthogonal codes as the single-user bound. Also the results in these

figures confirm that the performance of the space-time system with a single-user is only 3 dB far from the MRC with the same number of diversity branches. This 3 dB difference, relative to the MRC, is simply due to the fixed power constraint set at the transmitter side where two antennas are used. Furthermore, one can see from the results in Figures 4.1 and 4.2, the achieved diversity order of the underlying space-time system (i.e., NM=2,4 in Figures 4.1, 4.2 respectively) is independent of the system load. This quite clear from the slope of the BER results at high SNRs for different system loads.

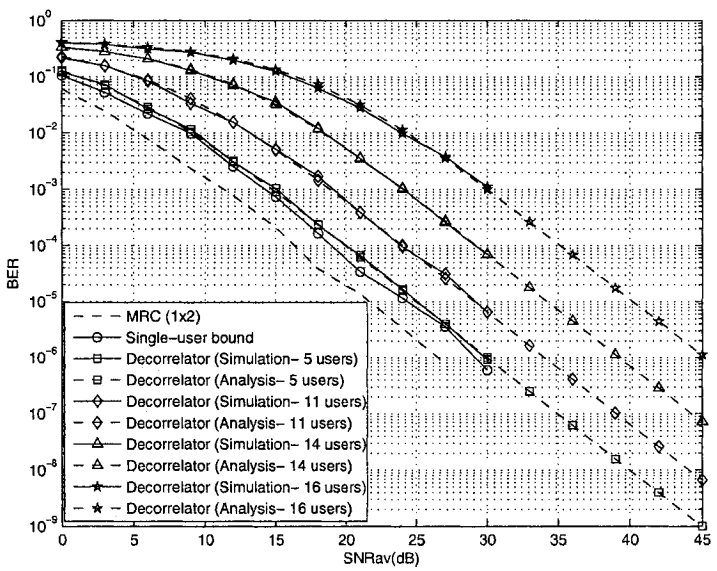

Figure 4.1: BER performance comparison for N=2, M=1 antennas for 1, 5, 11, 14 and 16 users over Rayleigh slow-fading channel.

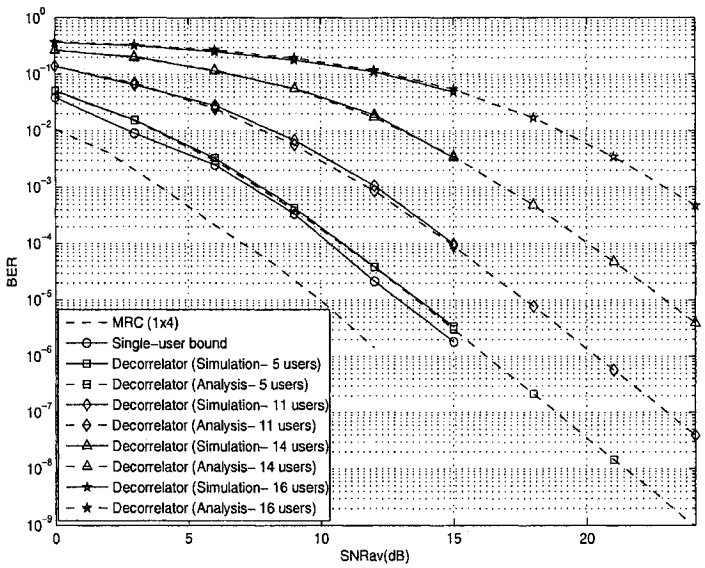

Figure 4.2: BER performance comparison for N=2, M=2 antennas for 1, 5, 11, 14 and 16 users over Rayleigh slow-fading channel.

4.5.2 Asymptotic Performance

In Figures 4.3, 4.4, we examine the accuracy of the asymptotic BER expression given in (4.25) for $N = 2$ and $M = 1$, $N = 2$ and $M = 2$ antenna configurations. As seen from these results, the BER approximation in (4.25) converges to the true BER at high SNRs. One should also note that the accuracy of this BER approximation is a function of the system load and hence the interference level. This is clear from the results in Figures 4.3 and 4.4 where the BER approximation converges to the true BER values at lower SNR for a system with smaller number of users than a one with a large number. This agrees well with our previous assumption $\bar{\gamma}_c \ggg C$ wherein the parameter C is a measure of the system interference.

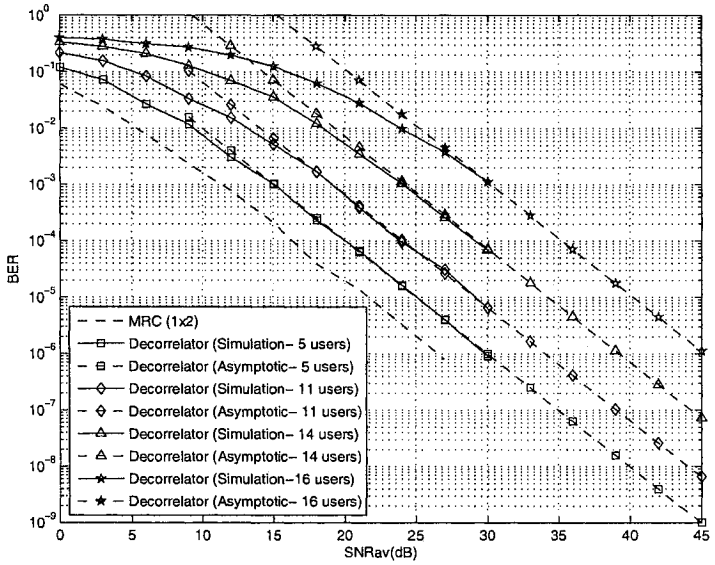

Figure 4.3: Asymptotic performance for N=2, M=1 antennas for 5, 11, 14 and 16 users over Rayleigh slow-fading channel.

Another important remark that can be deduced from (4.25) is that for different system loads, the BER degradation from the single-user bound is dependent on the system interference seen from the parameter C. In Table I, we quantify this SNR loss for systems with different number of users. From (4.25), this SNR loss is given by

$$\Delta_{\text{dB}} = 10 \log \left(\frac{C}{2} \right). \tag{4.26}$$

Table 4.1: Values of the parameters R_{11}^{-1}, R_{22}^{-1}, C and Δ for different system loads.

Number of users	R_{11}^{-1}	R_{22}^{-1}	C	Δ(dB)
5	1.0152	1.2948	2.31	0.6258
11	1.9006	4.033	5.9336	4.7229
14	13.7079	5.939	19.6469	9.9226

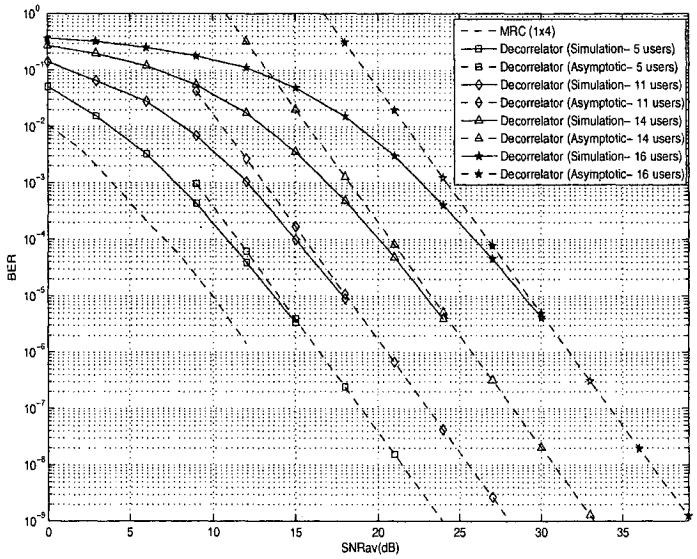

Figure 4.4: Asymptotic performance for N=2, M=2 antennas for 5, 11, 14 and 16 users over Rayleigh slow-fading channel.

Note that the values given in Table I are in a good agreement with the results in Figures 4.1-4.4. More importantly, as was noted from our analytical results in Section 4.4, this SNR degradation is not a function of the number of transmit and/or receive antennas.

As a final investigation, in Figure 4.5 we examine the performance of the space-time spreading scheme for a system with 11 users as a function of the number of receive antennas. We noted that these results are identical to a MRC receiver with the same number of diversity branches, but with 3 dB SNR loss.

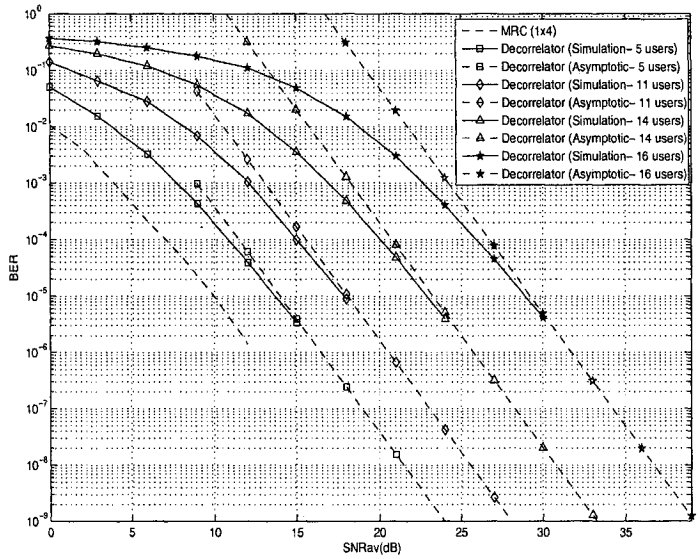

Figure 4.4: Asymptotic performance for N=2, M=2 antennas for 5, 11, 14 and 16 users over Rayleigh slow-fading channel.

Note that the values given in Table I are in a good agreement with the results in Figures 4.1-4.4. More importantly, as was noted from our analytical results in Section 4.4, this SNR degradation is not a function of the number of transmit and/or receive antennas.

As a final investigation, in Figure 4.5 we examine the performance of the space-time spreading scheme for a system with 11 users as a function of the number of receive antennas. We noted that these results are identical to a MRC receiver with the same number of diversity branches, but with 3 dB SNR loss.

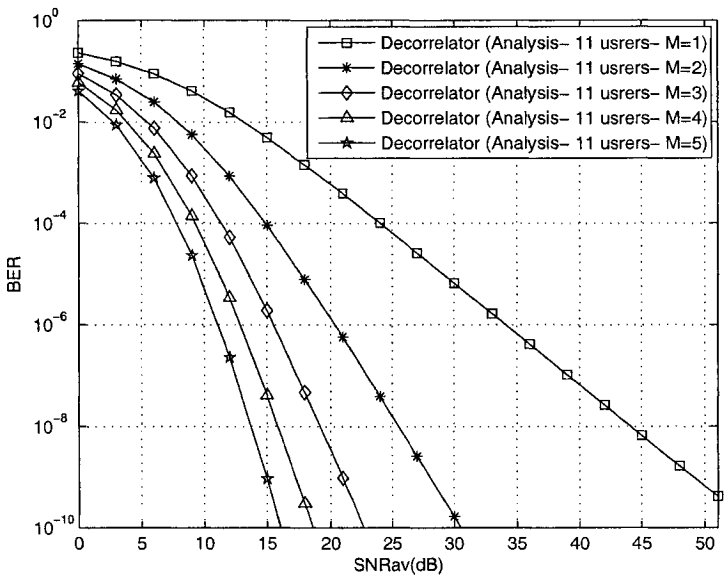

Figure 4.5: BER performance for a system with 11 users as a function of the number of receive antennas (M).

4.6 Conclusion

In this chapter, we investigated the performance of transmit diversity using space-time spreading in an uplink DS-CDMA system over slow-fading channels. We introduced an exact expression for the probability of bit error for $N = 2$ transmit and M receive antennas for a decorrelator based receiver. Using both simulation and analysis results, we proved that this scheme achieves the same diversity order as the MRC with the same number of diversity branches. More importantly, we proved that the diversity order of the underlying scheme is always maintained regardless of the system load. Moreover, we verified the accuracy of the derived probability of

error expression under different system parameters. Also, we developed an asymptotic expression for the probability of error at high average SNRs and justified its importance in systems with large number of users. Finally, and for the multiuser system, we have obtained a tight upper bound on the SNR loss from the single-user system. This bound was shown to be only a function of the system load and not the number of transmit or receive antennas.

Chapter 5

Conclusions and Future Works

5.1 Conclusions

This section briefly summarizes the accomplished work and the major contributions in this thesis.

1. We first, proposed a simple STBC transmit diversity scheme for DS-CDMA systems based on space-time spreading, that exploits both spatial and temporal diversities for fast-fading channels. We have proved that, with the same number of antennas as the MRC, the proposed coding scheme is able to achieve the full diversity promised by the channel (i.e., spatial and temporal). Also the effect of signal interference arising from the use of nonorthogonal codes was discussed. In that, we developed a simple adaptive decoder based on the NLMS algorithm that was shown to achieve the same diversity order as that

of the ideal orthogonal codes.

2. In Chapter 3, we studied the performance of the proposed scheme over fast-fading channels under different system loads for nonorthogonal spreading codes. It was shown that the diversity order offered is the same as the ideal orthogonal case. We also demonstrated that the performance of the adaptive MMSE preserves the same diversity order as that of the centralized MMSE receiver, but with small SNR degradation especially at high SNRs. Then we derived theoretical results for the probability of bit error for the single-user. For the multiuser system, we developed a semi-analytical model that provides a general representation of the performance analysis of the proposed space-time transmission scheme. By comparison with simulations the accuracy of this model was investigated in a DS-CDMA system using the decorrelator multiuser detector. We also obtained the pdf of the SIR through the transformation of random variables. By averaging over this pdf, we obtained the probability of bit error for the proposed scheme system with two transmit and M receive antennas. Using both simulation and analytical results we showed that for a system employing the decorrelator multiuser detector, the diversity order will be maintained irrespective of the system load.

3. In Chapter 4, we investigated the performance of the proposed scheme over slow-fading channels. We introduced an exact expression for the probability of bit error for $N = 2$ transmit and M receive antennas and for a decorrelator

based receiver. Using both simulation and analysis results, we proved that this scheme achieves the same diversity order as the MRC with the same number of diversity branches. More importantly, we proved that the diversity order of this scheme is always maintained regardless of the system load. Moreover, we verified the accuracy of the derived probability of error expression under different system parameters. Also, we developed an asymptotic expression for the probability of error at high average SNRs and justified its importance in systems with large number of users. Finally, and for the multiuser system, we have obtained a tight upper bound on the SNR loss from the single-user system. This bound was shown to be only a function of the system load and not the number of transmit or receive antennas.

5.2 Future Works

We address in what follows some topics of interest for the future extension of this research.

1. In this work, we assumed that the receiver has perfect knowledge of the spreading sequences and channel coefficients for all users. However, this may not be true in practice. Thus, future studies should investigate the effect of imperfect channel state information on the receiver performance. In addition, throughout this work we assumed a synchronous CDMA system, which is ideally optimistic. Therefore, this study should be carried over an asynchronous

DS-CDMA system to investigate the performance of the receiver with timing and code inaccuracies.

2. On the other hand, the research conducted in Chapter 3 and 4 has focused on the study of the performance of the proposed scheme over flat-fading channels. Hence, to represent a more practical system, this research should involve the study of the performance of the proposed scheme over frequency-selective fading channels using the Rake receiver.

3. Through out this thesis it has been assumed that the receiver has perfect knowledge of channel path gains, which seem unrealistic specially for fast-fading scenarios. Thus, in future, system performance should be investigated considering unknown path gains at the receiver, *i.e.* non-coherent detection. This study should address the effect of imperfectly estimated path gains especially in rapidly changing environments on the receiver performance.

Appendix A

The integral in (3.57) over β_1 involves two integrations denoted by I_{1,β_1} and I_{1,β_2}. The I_{1,β_1} integration is given by

$$I_{1,\beta_1} = \int_0^\infty C_2^{(4M+k+j+1)} \beta_1^{(8M-1)} e^{-\beta_1^2 \mu_2} \; {}_1F_1\left(1; 4M+k+j+2; \frac{C_2\beta_1^2}{2\sigma^2}\right) d\beta_1 \qquad \text{(A.1)}$$

where $\mu_2 = \frac{2\sigma^2 + C_2 N_o \sin^2\theta}{2\sigma^2 N_o \sin^2\theta}$. The integration in $(A.1)$ can be evaluated using [43, (7.621.4)]

$$\int_0^\infty e^{-st} t^{b-1} \; {}_1F_1(a; c; kt) dt = \Gamma(b)(s-k)^{-b} \times \; {}_2F_1\left(c-a, b; c; \frac{k}{k-s}\right). \qquad \text{(A.2)}$$

By introducing the substitution $r = \beta_1^2$, $(A.1)$ reduces to

$$\begin{aligned} I_{1.\beta_1} &= \int_0^\infty C_2^{(4M+k+j+1)} r^{(4M-1)} e^{-r\mu_2} \; {}_1F_1(1; 4M+k+j+2; \frac{c_2 r}{2\sigma^2}) dr \\ &= C_2^{(4M+k+j+1)} \Gamma(4M) \left(\frac{\sin^2\theta}{\bar{\gamma}_c}\right)^{4M} \; {}_2F_1(4M+k+j+1, 4M; 4M+k+j+2; -\frac{C_2 \sin^2\theta}{\bar{\gamma}_c}) \end{aligned} \qquad \text{(A.3)}$$

where ${}_2F_1(.,.;.;.)$ is the hypergeometric function of the second kind. In a similar way, one can show that

$$I_{2,\beta_1} = \int_0^{\infty} C_1^{(4M+k+j+1)} r^{(4M-1)} e^{-r\mu_1} \; {}_1F_1(1; 4M+k+j+2; \frac{C_1 r}{2\sigma^2}) dr$$

$$= C_1^{(4M+k+j+1)} \Gamma(4M) \left(\frac{\sin^2\theta}{\bar{\gamma}_c}\right)^{4M} \; {}_2F_1(4M+k+j+1, 4M; 4M+k+j+2; -\frac{C_1 \sin^2\theta}{\bar{\gamma}_c}) \tag{A.4}$$

where $\mu_1 = \frac{2\sigma^2 + C_1 N_o \sin^2\theta}{2\sigma^2 N_o \sin^2\theta}$.

By rewriting (3.57) after combining $(A.3)$ and $(A.4)$, we obtain

$$P_b = \frac{\lambda}{\pi} \sum_{k=0}^{2M-1} \sum_{j=0}^{2M-1} \frac{(-1)^{k+j}}{4M+k+j+1} \binom{2M-1}{k} \binom{2M-1}{j} C_2^{2M-k-1} C_1^{2M-j-1} \Gamma(4M)$$

$$\int_0^{\frac{\pi}{2}} \left(\frac{\sin^2\theta}{\bar{\gamma}_c}\right)^{4M} \left[C_2^{4M+k+j+1} \; {}_2F_1\left(4M+k+j+1, 4M; 4M+k+j+2; -\frac{C_2 \sin^2\theta}{\bar{\gamma}_c}\right) \right.$$

$$\left. - C_1^{4M+k+j+1} \; {}_2F_1\left(4M+k+j+1, 4M; 4M+k+j+2; -\frac{C_1 \sin^2\theta}{\bar{\gamma}_c}\right) \right] d\theta. \tag{A.5}$$

Now, the integral in $(A.5)$ over θ also involves two parts denoted by $I_{1,\theta}$ and $I_{2,\theta}$. The first integration can be expressed as

$$I_{1,\theta} = \int_0^{\frac{\pi}{2}} \left(\sin^2\theta\right)^{4M} C_2^{(4M+k+j+1)} \; {}_2F_1\left(4M+k+j+1, 4M; 4M+k+j+2; -\frac{C_2 \sin^2\theta}{\bar{\gamma}_c}\right) d\theta \tag{A.6}$$

which can be solved using [44, (7.512.12)]

$$\int_0^1 x^{v-1}(1-x)^{\mu-1}\ {}_pF_q(a_1,.....,a_p;b_1,.....,b_q;ax)dx$$
$$= \frac{\Gamma(\mu)\Gamma(v)}{\Gamma(\mu+v)}\ {}_{p+1}F_{q+1}(v,a_1,.....,a_p;\mu+v,b_1,.....,b_q;a). \tag{A.7}$$

By introducing the substitution $w = \sin^2\theta$, and using $(A.6)$, $(A.7)$ will reduce to

$$I_{1,\theta} = \int_0^1 C_2^{(4M+k+j+1)} w^{(4M-\frac{1}{2})}(1-w)^{-\frac{1}{2}}$$
$${}_2F_1\left(4M+k+j+1,4M;4M+k+j+2;-\frac{C_2 w}{\bar{\gamma}_c}\right)dw$$
$$= \frac{\Gamma(4M+\frac{1}{2})\Gamma(\frac{1}{2})}{\Gamma(4M+1)} C_2^{(4M+k+j+1)}$$
$${}_3F_2\left(4M+\frac{1}{2},4M+k+j+1,4M;4M+1,4M+k+j+2;-\frac{C_2}{\bar{\gamma}_c}\right). \tag{A.8}$$

Similarly, one can show that

$$I_{2,\theta} = \int_0^1 C_1^{(4M+k+j+1)} w^{(4m-\frac{1}{2})}(1-w)^{-\frac{1}{2}}$$
$${}_2F_1\left(4M+k+j+1,4M;4M+k+j+2;-\frac{C_1 w}{\bar{\gamma}_c}\right)dw$$
$$= \frac{\Gamma(4M+\frac{1}{2})\Gamma(\frac{1}{2})}{\Gamma(4M+1)} C_1^{(4M+k+j+1)}$$
$${}_3F_2\left(4M+\frac{1}{2},4M+k+j+1,4M;4M+1,4M+k+j+2;-\frac{C_1}{\bar{\gamma}_c}\right). \tag{A.9}$$

Finally, substitution of $(A.8)$ and $(A.9)$ into $(A.5)$ yields to the probability of error expression in (3.58).

Bibliography

[1] R. Pickholtz, D. Schilling, L. Milestein, "Theory of spread-spectrum communications-A tutorial," IEEE Trans. Communications, pp. 855-884, May. 1982.

[2] W. Firmanto, B. Vucetic, and J. Yuan, "Space-time TCM with improved performance on fast fading channels," *IEEE Commun. Letters*, vol. 5, no. 4, pp. 154156, Apr. 2001.

[3] V. Tarokh, N. Seshadri, and A. R. Calderbank, "Space-time codes for high data rate wireless communication: Performance criterion and code construction," *IEEE Trans. Inform. Theory*, vol. 44, pp. 744765, March 1998.

[4] S. M. Alamouti, "A simple transmit diversity technique for wireless communications," *IEEE J. Select. Areas Commun.*, vol. 16, no. 8, pp. 14511458, Oct. 1998.

[5] B. Hochwald, T. Marzetta, and C. Papadias, "A transmitter diversity scheme for wideband CDMA systems based on space-time spreading," *IEEE J. Select. Areas Commun.*, vol. 19, no. 1, pp. 4860, Jan. 2001.

[6] S. Verdú, Multiuser Detection, Cambridge University Press, 1998.

[7] A. J. Paulraj and C. B. Papadias, "Space-time processing for wireless communications," *IEEE Signal Processing Mag.*, vol. 14, pp. 49-83, Nov. 1997.

[8] J. G. Proakis, Digital Communications, 3rd ed., New York: Mc-Graw-Hill, 1995.

[9] S. Verdú, "Minimum probability of error for asynchronous multiple-access comunication systems," *in Proc. 1983 IEEE Military Communications Conf.*, Mov. 1983, vol. 1, pp. 213-219.

[10] S. Moshavi, "Multiuser Detection for DS-CDMA communications," *IEEE Commun. Mag.*, vol. 34, pp. 24-136, October 1996.

[11] K. Schneider, "Optimum detection of code divison multiplexed signals," *IEEE Tran. Aerospace and Electronic Systems*, vol. AES-15, pp. 181-185, Jan. 1979.

[12] R. Kohno, H. Imai, and M. Hatori, "Cancellation techniques of co-channel interference in asynchronous spread spectrum multiplex access systems," *Electronics and Communications*, vol. 66-A, pp. 20-29, 1983.

[13] R. Lupas and S. Verdú, "Near-far resistance of multiuser detection in asynchronous channels," *IEEE Trans. Commun.*, vol .38, pp. 496-508, Apr. 1990.

[14] R. Lupas and S. Verdú, "Linear multiuser detectors for synchronous code-division multiple-access channels," *IEEE Trans. Inform. Theory*, vol. 35, pp. 123-136, Jan. 1989.

[15] R. Iltis and L. Mailaender, "Multiuser detection of quasi-synchronous CDMA signals using linear decorrelators," IEEE Trans. Commun., vol. 44, pp. 1561-1571, Nov. 1996.

[16] Z. Xie, R. T. Short, and C. T. Rushforth, "A family of suboptimum detectors for coherent multiuser communications," *IEEE J. Select. Areas Commun.*, vol. 8, pp. 683-690, May 1990.

[17] J. Yang and S. Roy, "On joint transmitter and receiver optimization for multiple-input-multiple-output (MIMO) transmissions," *IEEE Trans. Commun.*, vol. 42, Dec. 1994.

[18] H. V. Poor and S. Verdú, "Probability of error in MMSE multiuser detection," *IEEE Trans. Inform. Theory*, vol. 43, pp. 858-871, May 1997.

[19] S. L. Miller, "An adaptive direct-sequence code-divion multiple-access receiver for multiuser interference rejection," *IEEE Tran. Commun.*, vol. 43, pp.1746-1755, Feb./Mar./Apr. 1995.

[20] P. B. Rapajic and B. S. Vucetic, "Adaptive receiver structures for asynchronous CDMA systems," *IEEE J. Select. Areas Commun.*, vol. 12, pp. 685-697, May. 1994.

[21] S. Verdú, "Adaptive multiuser detection," *in Proc. IEEE Int. Symp. on Spread Spectrum Theory and Applications*, July. 1994.

[22] U. Madhow, L. M. Honig, "MMSE interference suppression for Direct-Sequence Spread-Spectrum CDMA," *IEEE Tran. Commun.*, vol. 42, pp. 3178-3188, Dec. 1994.

[23] M. Abdulrahman, D. D. Falconer, and A. U. H. Sheikh, "Equalization for interference cancellation in spread-spectrum multiple-access systems," *Proc. of IEEE VTC*, pp. 71-74, 1992.

[24] M. L. Honig, U. Madhow, and S. Verdu, "Blind adaptive multiuser detection," *IEEE Trans. Inform. Theory*, vol. 41, pp. 944-960, July 1995.

[25] M. L. Honig and M. K. Tsatsanis, "Adaptive techniques for multiuser CDMA receivers", *IEEE Signal Processing Magazine*, vol. 17, pp. 49-61, May 2000.

[26] V. Tarokh, H. Jafarkhani, and A. Calderbank, "Space-time block codes from orthogonal designs," *IEEE Trans. Inform. Theory*, vol. 45, pp. 1456-1467, July 1999.

[27] G. Foschini and M. Gans, "On limits of wireless communication in a fading environment when using multiple antennas," *Wireless Personal Communications*, vol. 6, pp. 311-335, March 1998.

[28] X. Lin and R. S. Blum, "Improved space-time codes using serial concatenation," *IEEE Commun. Letters*, vol. 4, no. 7, pp. 221–223, July 2000.

[29] S. M. Alamouti, V. Tarokh, and P. Poon, "Trellis-coded modulation and transmit diversity: design criteria and performance evaluation," *in Proc. ICUCP*, 1998.

[30] S. Sandhu, R. Heath, and A. Paulraj, "Space-time block codes versus space-time trellis codes," *in Proc., IEEE Inter. Conf. on Commun.*, (ICC2001), vol. 4, pp. 1132-1136, June 2001.

[31] Y. Liu, M. P. Fitz, and O. Y. Takeshita, "Full rate space-time turbo codes," *IEEE J. Select. Areas Commun.*, vol. 19, no. 5, pp. 969-980, May 2001.

[32] W. Hamouda and A. Ghrayeb, "Performance of convolutionally-coded MIMO systems with antenna selection," *J. of Commun. and Networks*, vol. 7, no. 3, pp. 307-312, Sept. 2005.

[33] J. C. Guey, "Concatenated coding for transmit diversity systems," *in Proc., IEEE Veh. Technol. Conf.*, vol. 5, pp. 2500-2504, Fall 1999.

[34] S. Baro, G. Bauch, and A. Hansmann, "Improved codes for space-time trellis-coded modulation," *IEEE Commun. Letters*, vol. 4, no. 1, pp. 2022, Jan. 2000.

[35] S. Jayaweera and H.V. Poor, "A Rake-based iterative receiver for space-time block-coded multipath CDMA," *IEEE Trans. Signal Processing*, vol. 52, pp. 796-806, Mar. 2004.

[36] W. Hamouda, "Space-time spreading for MIMO CDMA-based systems over fast-fading channels," *Proc. 2005 IEEE Int. Conf., Wireless Networks, Comm. and Mobile Comp.*, 2005.

[37] W. Hamouda and M. AlJerjawi, "A Transmit Diversity Scheme using Space-Time Spreading for DS-CDMA Systems in Fast-Fading Channels," *IEEE Veh. Technol. Conf.*, Fall 2005.

[38] M. Latva-aho and M. Juntti, "MMSE detection of DS-CDMA systems in fading channels," *IEEE Trans. Commun.*, vol. 48, no. 2, pp. 194–199, Feb. 2000.

[39] S. Jayaweera and H.V. Poor, "Low complexity receiver structures for space-time coded multiple-access systems," *EURASIP J. Applied Signal Processing (special Issue on Space-Time Coding)*, pp. 275-288, Mar. 2002.

[40] M. AlJerjawi and W. Hamouda, "Performance of Space-Time Spreading in Multiuser DS-CDMA Systems over Fast-Fading Channels", *Proc. 2005 IEEE Global Telecommunications Conference*, Nov./Dec. 2005.

[41] A. Papoulis, Probability, Random Variables, and Stochastic Processes. McGraw-Hill, Inc. 1991.

[42] M. Abramowitz and I. A. Stegun, Handbook of Mathematical Functions with Formulas, Graphs, and Mathematical Tables, New York: Dover, 1964.

[43] M. K. Simon and M. Alouini, "A unified approach to the performance analysis of digital communication over generalized fading channels", *Proc. of the IEEE*, vol. 86, pp. 1860 - 1877, Sept. 1998.

[44] I. S. Gradshteyn and I. M. Ryzhik, Table of Integrals, Series and Products, 5thEd., New York: Academic, 1995.

[45] M. AlJerjawi and W. Hamouda, "Performance Analysis of Space-Time Diversity in Multiuser CDMA Systems over Rayleigh Fading Channels," *Proc. IEEE International Conference on Communications (ICC 2006)*, Istanbul, Turkey, June 2006.

[46] L. Zhu and U. Madhow, "Adaptive interference suppression for direct sequence CDMA over severly time-varying channels," *in Proc. 1997 GLOBECOM*, pp. 917922.

[47] R. Schober, W. Gerstacker, and A. Lampe, "Noncoherent MMSE interference suppression for DS-CDMA," *in IEEE International Conference on Communications (ICC 2001)*, Helsinki, Finland, June 2001.

[48] Y. J. Kou, W. -S. Lu, and A. Antoniou, "Application of space-time block coding in DS-CDMA communication systems," *Proc. IEEE Commun., Computers and signal Processing Conf., PACRIM 2001*, vol. 1, 2001, pp. 132-135.

[49] Y.-H. Jung, S.-C. Hong, S. R. Kim, and Y. H. Lee, "Adaptive CMMSE receivers for space-time block coded MIMO CDMA systems," *Proc. IEEE Vehicular Technology Conference, VTC 2002, Vancouver, Canada*, 2002, pp. 8-12.

[50] H. Huang and H. Viswanathan, "Multiple antennas and multiuser detection in high data rate CDMA systems," *IEEE Vehicular Technology Conference, Tokyo, Japan*, 2000, pp. 556-560.

[51] Chul-Seung Lee, Dong-Jun Cho, Mi-Jeong Kim, Young-Hwan You and Hyoung-Kyu Song, "Performance of Space-Time Block Code for DS-CDMA UWB System," *Proceedings of ICCE 2005*, p. 349-350, 8-12 Jan. 2005.

[52] Ping-Hung Chiang, Hsueh-Jyh Li and Ding-Bing Lin, "Performance analysis of two-branch space-time block coded DS-CDMA systems in time-varying multipath Rayleigh fading channels," *IEEE International Symposium on Spread Spectrum Techniques and Applications*, p. 130-134, 30 Aug.-2 Sept. 2004.

[53] W. Li, T.A. Gulliver and W. Chow, "A new SIC algorithm for STBC coded DS-CDMA systems," *Proceedings of the IEEE 6th Circuits and Systems Symposium on Emerging Technologies: Frontiers of Mobile and Wireless Communication*, vol. 1, p. 357-360, 2004.

[54] X. Yue, W. Zhu and H. Fan, "Space-time coded CDMA: blind equalization and multiuser detection," *Conference on Signals, Systems and Computers*, vol. 1, p. 607-611, 7-10 Nov. 2004.